J. Fluid Mech. (1993), *vol.* 252, *pp.* 419–448

Instability of stratified fluid in a vertical cylinder†

By G. K. BATCHELOR[1] AND J. M. NITSCHE[2]

[1] Department of Applied Mathematics and Theoretical Physics, University of Cambridge, Silver Street, Cambridge CB3 9EW, UK

[2] Department of Chemical Engineering, State University of New York at Buffalo, Buffalo, NY 14260, USA

(Received 31 July 1992 and in revised form 4 February 1993)

In a previous paper we analysed the stability to small disturbances of stationary stratified fluid which is unbounded. Various forms of the undisturbed density distribution were considered, including a sinusoidal profile and a function of the vertical coordinate z which is constant outside a central horizontal layer. Both these types of stratification are so unstable that the critical Rayleigh number is zero. In this sequel we make the study more complete and more useful by taking account of the effect of a vertical circular cylindrical boundary of radius a which is rigid and impermeable. As in the previous paper we assume that the undisturbed density distribution is steady.

The case of fluid in a vertical tube with a uniform density gradient is useful for comparison, and so we review and extend the available results, in particular obtaining growth rates for a disturbance which is neither z-independent nor axisymmetric. A numerical finite-difference method is then developed for the case in which $\mathrm{d}\rho/\mathrm{d}z = \rho_0 \kappa A \cos \kappa z$. When $\kappa a \ll 1$ the relation between growth rate and Rayleigh number approximates to that for a uniform density gradient of magnitude $\rho_0 \kappa A$; and when $\kappa a \gg 1$ the tilting–sliding mechanism identified in the previous paper is relevant and the results approximate to those for an unbounded fluid, except that the smallest Rayleigh number for a neutral disturbance is not zero but is of order $(\kappa a)^{-1}$. In the case of an undisturbed density which varies only in a central layer of thickness l, the same mechanism is at work when the horizontal lengthscale of the disturbance is large compared with l, resulting in high growth rates and a critical Rayleigh number which vanishes with l/a. Estimates of the growth rate are given for some particular density profiles.

1. Introduction

This paper is a sequel to the study of instability of stationary stratified fluid described in our earlier publication (Batchelor & Nitsche 1991, to be referred to as BN1). In that paper we considered the behaviour of small disturbances to unbounded fluid with vertical density profiles of unconventional form. In one particular case the profile was sinusoidal and in another the fluid density was uniform except in a central layer. Surprisingly, the fluid is so unstable in these two cases (regardless of the distribution of density within the central layer in the second case) that for sufficiently small horizontal wavenumber there exists a neutral disturbance, however small the Rayleigh number. Disturbances with large horizontal lengthscale are efficient in releasing potential energy, and large-scale tilting and relative sliding of the initially horizontal plane layers of heavy or light fluid is an especially effective mechanism.

† With an appendix by M. R. E. Proctor.

The focus in the previous paper was on the novel undisturbed density profiles, and for simplicity it was assumed that no boundaries are present. Here we give the investigation more practical relevance by supposing that the fluid is contained within a vertical cylinder whose cross-section is circular. Horizontal boundaries are again absent. Disturbances with indefinitely large horizontal lengthscale are excluded by the presence of the boundary, and so a non-zero critical wavenumber may be expected. Our general purpose is to clarify the mechanical processes involved in the growth of small disturbances and to obtain quantitative information about the effect of rigid insulating containing walls.

The specific vertical distributions of density in the undisturbed fluid that we shall consider are as follows:

(i) uniform density gradient;

(ii) sinusoidal density variation;

(iii) uniform density outside a central layer.

Publications on the classical case (i) go back over a number of years, and we include it within the scope of this paper mainly for purposes of comparison. However, the available results for the instability of fluid with a uniform gradient in a vertical cylinder are by no means complete and some new developments will be presented here. The case of fluid with a sinusoidal distribution of density, now in a vertical tube of circular cross-section, is again our primary concern owing to its potential application to the secondary instability of a fluidized bed (Batchelor 1991). A number of interesting results were found in BN1 for the third type of density distribution, in which variations are confined to a central layer, and we shall enquire here whether and how they are modified by the presence of a cylindrical boundary.

As in BN1 the fluid is assumed to be viscous and incompressible, and the conserved physical quantity that determines the density of the fluid (e.g. mass of a solute in liquid) is transported with a molecular diffusivity D. Note that we again suppose that the effect of diffusion on the density distribution in the undisturbed state may be ignored, so that an undisturbed state in which the fluid is stationary and the density varies only in the vertical direction is *steady*. This convenient assumption cannot be justified generally, except of course when $D = 0$ or the undisturbed density gradient is uniform, but it is allowable in some particular circumstances which are readily recognized when the behaviour of small disturbances of different kinds has been analysed. For example, the Rayleigh number for a neutral disturbance of small horizontal wavenumber in unbounded fluid whose density is uniform except in a central layer is found to depend primarily on the total excess mass of the layer per unit area of the horizontal plane, and this quantity is unchanged by diffusion.

After setting out the disturbance equations in §2 and noting the simple structure of the problem when $\nu = 0, D = 0$, we shall consider in turn the three types of density distribution in the undisturbed state in §§3, 4 and 5. Section 6 is a resumé of what we have found in the two papers together.

2. The disturbance equations and boundary conditions

The notation here is exactly the same as in BN1. It was shown in that paper that the linearized equations for the small disturbance quantities $\boldsymbol{u}, \rho', p'$ are as follows:

$$\nabla \cdot \boldsymbol{u} = 0, \tag{2.1}$$

$$\frac{\partial \boldsymbol{u}}{\partial t} = \frac{\rho' \boldsymbol{g}}{\rho_0} - \frac{\nabla p'}{\rho_0} + \nu \nabla^2 \boldsymbol{u}, \tag{2.2}$$

$$\frac{\partial \rho'}{\partial t} + w\frac{\mathrm{d}\rho_1}{\mathrm{d}z} = D\nabla^2\rho', \tag{2.3}$$

in which the vertical coordinate z and the corresponding velocity component w are positive upwards and $\rho_0 + \rho_1(z)$ is the fluid density in the steady undisturbed state, the variable part ρ_1 being small compared with ρ_0 in order to allow use of the Boussinesq approximation and a linear relation between fluid density and solute concentration (or similar quantity). It is possible by manipulation of these equations to obtain the well-known equation containing only the one dependent variable w, namely

$$\left(\frac{\partial}{\partial t} - D\nabla^2\right)\left(\frac{\partial}{\partial t} - \nu\nabla^2\right)\nabla^2 w = \frac{g}{\rho_0}\frac{\mathrm{d}\rho_1}{\mathrm{d}z}\nabla_h^2 w, \tag{2.4}$$

where the suffix h means 'in the horizontal plane'. Once w has been found, the other disturbance quantities ρ', p' and $\boldsymbol{u}_h$ are given respectively by (2.3) and

$$\nabla^2 p' = \boldsymbol{g}\cdot\boldsymbol{\nabla}\rho' \tag{2.5}$$

and

$$\left(\frac{\partial}{\partial t} - D\nabla^2\right)\left(\frac{\partial}{\partial t} - \nu\nabla^2\right)\nabla^2\boldsymbol{u}_h = -\frac{g}{\rho_0}\frac{\partial}{\partial z}\left(\frac{\mathrm{d}\rho_1}{\mathrm{d}z}\boldsymbol{\nabla}_h w\right). \tag{2.6}$$

We suppose that the fluid is contained within a vertical cylinder with a rigid impermeable circular boundary of radius a. The boundary conditions to be satisfied by the disturbance are then

$$w = 0, \quad \partial\rho'/\partial r = 0, \quad \boldsymbol{u}_h = 0 \quad \text{at} \quad r = a \text{ for all } z, \tag{2.7}$$

where r is the horizontal distance from the cylinder axis.

It will be assumed that normal modes exist, in which case

$$w, \rho', \boldsymbol{u}_h \propto \mathrm{e}^{\gamma t} \tag{2.8}$$

and (2.4) becomes

$$\left(\frac{\gamma}{D} - \nabla^2\right)\left(\frac{\gamma}{\nu} - \nabla^2\right)\nabla^2 w = \frac{g}{D\nu\rho_0}\frac{\mathrm{d}\rho_1}{\mathrm{d}z}\nabla_h^2 w. \tag{2.9}$$

The inviscid diffusionless limit

The above system of equations and boundary conditions becomes much simpler in the limit $\nu \to 0, D \to 0$. There are circumstances in which the disturbance Reynolds number $\gamma l^2/\nu$ and the corresponding Péclet number $\gamma l^2/D$ (where l is a length characteristic of the disturbance) are large, and it is worthwhile therefore to examine this limit. In this preliminary section we formulate the stability problem for a fluid with $\nu = 0$ and $D = 0$ for later use. In this case, (2.9) for w reduces to

$$\nabla^2 w = \frac{g}{\gamma^2\rho_0}\frac{\mathrm{d}\rho_1}{\mathrm{d}z}\nabla_h^2 w. \tag{2.10}$$

A solution such that w is of the separable form

$$w = \mathrm{e}^{\gamma t} W(z)\, F(\boldsymbol{x}_h) \tag{2.11}$$

then exists provided

$$\nabla^2 F = -\alpha^2 F, \quad \frac{\mathrm{d}^2 W}{\mathrm{d}z^2} + \alpha^2 W\left(\frac{g}{\gamma^2\rho_0}\frac{\mathrm{d}\rho_1}{\mathrm{d}z} - 1\right) = 0, \tag{2.12a, b}$$

where $\boldsymbol{x}_h$ is the horizontal component of the position vector and α is a generalized

wavenumber parameter. The magnitude of W is arbitrary, but F will be normalized by the convenient relationship

$$\frac{1}{S}\int F^2\,\mathrm{d}S = \tfrac{1}{2}, \tag{2.13}$$

where S is the area of the cross-section of the containing cylinder. The corresponding expression for $\boldsymbol{u}_h$ is seen from (2.1) to be

$$\boldsymbol{u}_h = \mathrm{e}^{\gamma t}\alpha^{-2}\frac{\mathrm{d}W}{\mathrm{d}z}\nabla F. \tag{2.14}$$

The one surviving boundary condition at a rigid cylindrical wall is

$$\partial F/\partial r = 0 \quad \text{at} \quad r = a, \tag{2.15}$$

and this serves to determine the generalized wavenumber α.

Equation (2.12a) and the boundary condition (2.15) are satisfied by

$$F(\boldsymbol{x}_h) = cJ_n(\alpha r)\cos n\theta, \quad J_n'(\alpha a) = 0, \tag{2.16a, b}$$

where (r, θ) are the polar coordinates in the horizontal plane and according to (2.13) c is given by

$$c^{-2} = \frac{2}{\pi a^2}\int_0^{2\pi}\int_0^a J_n^2(\alpha r)\cos^2 n\theta\, r\,\mathrm{d}r\,\mathrm{d}\theta = \left(1-\frac{n^2}{\alpha^2 a^2}\right)J_n^2(\alpha a) \tag{2.17}$$

on making use of the known integral properties of Bessel functions. There is an infinite set of values of αa satisfying (2.16b) for each of the infinite set of integral values of n, and the smallest permissible value of αa is of order unity.

The remaining task is to calculate the growth rate γ in terms of α as an eigenvalue of (2.12b) for $W(z)$. However, we cannot go further without specifying the vertical distribution of density in the undisturbed state. We note that (2.12b) for W also governs the behaviour of a disturbance in unbounded and inviscid diffusionless fluid which varies sinusoidally in a horizontal direction with arbitrary wavenumber α (this being a single Fourier component with respect to x).

The case of unbounded inviscid diffusionless fluid whose density is either sinusoidal in z or uniform outside a thin central layer was considered briefly in §7 of BN1, and later we shall supplement (and correct) that previous calculation of growth rates in view of the new-found generality of the results.

3. A uniform density gradient in the undisturbed state

In this case $\mathrm{d}\rho_1/\mathrm{d}z$ is constant, and (2.9) becomes a homogeneous linear equation with constant coefficients to which eigenvalue analysis of conventional form is applicable. A number of results for the growth of small disturbances to fluid in a vertical cylinder of circular or rectangular cross-section have been published, and we shall review and extend those relating to a circular cylinder before discussing cases of non-uniform density gradient in the later sections.

3.1. *General analysis*

A disturbance of arbitrary form may be Fourier-analysed with respect to z here, and the different Fourier components do not interact. It is sufficient therefore to consider a disturbance of the form

$$w = \mathrm{e}^{\gamma t}\cos\kappa z\, F(\boldsymbol{x}_h), \quad \rho' \propto \cos\kappa z, \quad \boldsymbol{u}_h \propto \sin\kappa z. \tag{3.1}$$

Equation (2.9) then reduces to

$$\left(\frac{\gamma}{D}-\nabla^2+\kappa^2\right)\left(\frac{\gamma}{\nu}-\nabla^2+\kappa^2\right)(\nabla^2-\kappa^2)F=\frac{g}{D\nu\rho_0}\frac{\mathrm{d}\rho_1}{\mathrm{d}z}\nabla^2 F. \tag{3.2}$$

If there were no boundaries present the problem would be completed by putting $F\propto\sin\alpha x$ and solving explicitly the resulting quadratic equation for the growth rate γ (see BN1, §3). When cylindrical walls are present we may proceed by observing that any solution of

$$\nabla^2 F=-\alpha^2 F \tag{3.3}$$

is also a solution of (3.2) provided α^2 satisfies the equation

$$\left(\frac{\gamma}{D}+\alpha^2+\kappa^2\right)\left(\frac{\gamma}{\nu}+\alpha^2+\kappa^2\right)(\alpha^2+\kappa^2)=\frac{\alpha^2 g}{D\nu\rho_0}\frac{\mathrm{d}\rho_1}{\mathrm{d}z}. \tag{3.4}$$

The equation (3.4) in general will yield three roots for α^2 and so three independent solutions for w of the form (3.1). There are three corresponding solutions for ρ', found from (2.3), and for $\boldsymbol{u}_h$, found from (2.6). However, there are four scalar boundary conditions in (2.7) to be satisfied, and it is not obvious where the required fourth independent solution comes from. There is no difficulty when the disturbance motion is two-dimensional or axisymmetric, since there are then only three scalar boundary conditions; nor is there any difficulty when $\kappa=0$ and the disturbance streamlines are vertical everywhere, because there are then only two independent solutions of (3.4) for α^2 and only two boundary conditions. Each of the cases of uniformly stratified fluid in a vertical circular cylinder with no-slip impermeable walls for which a solution has been found hitherto is in fact subject to one of these restrictions.

The missing independent solution is a *complementary function* of (2.6) for $\boldsymbol{u}_h$. The expression

$$\boldsymbol{u}_h=\mathrm{e}^{\gamma t}\sin\kappa z\,\boldsymbol{g}\times\nabla\hat{F}(\boldsymbol{x}_h) \tag{3.5}$$

represents a motion in the horizontal plane which satisfies (2.1)–(2.3) with w, ρ' and p' equated to zero provided $\hat{F}(\boldsymbol{x}_h)$ satisfies

$$\left(\frac{\partial}{\partial t}-\nu\nabla^2\right)(\mathrm{e}^{\gamma t}\sin\kappa z\,\boldsymbol{g}\times\nabla\hat{F})=0.$$

Thus (3.5) is an independent solution of the governing equations when

$$\nabla^2\hat{F}=(\kappa^2+\gamma/\nu)\,\hat{F}. \tag{3.6}$$

This fourth independent solution describes a distribution of vorticity generated at a vertical rigid boundary, and is zero for geometrical reasons when the disturbance is axisymmetric or z-independent. The need to take account of the vertical vorticity generated at the boundary in a similar stability problem with stress-free boundary conditions has been noted by Jones & Moore (1979).

An appropriate solution of (3.3) for the function F in the case of a circular cylindrical boundary is

$$F(\boldsymbol{x}_h,\alpha)=CJ_n(\alpha r)\cos n\theta,$$

where r,θ,z are cylindrical coordinates, C is an arbitrary constant and n is the azimuthal mode number. There are three roots of (3.4) for α^2, say $\alpha_1^2,\alpha_2^2,\alpha_3^2$, whence the general expression for the vertical velocity component w is

$$w=\mathrm{e}^{\gamma t}\cos\kappa z\cos n\theta\sum_{p=1}^{3}C_p J_n(\alpha_p r). \tag{3.7}$$

The corresponding expression for ρ' is seen from (2.3) to be

$$\rho' = -\mathrm{e}^{\gamma t}\cos\kappa z\cos n\theta\frac{\mathrm{d}\rho_1}{\mathrm{d}z}\sum_{p=1}^{3}\frac{C_p J_n(\alpha_p r)}{\gamma + D(\alpha_p^2+\kappa^2)}, \tag{3.8}$$

and that for the particular integral of (2.6) is

$$\boldsymbol{u}_h^{(1)} = -\mathrm{e}^{\gamma t}\sin\kappa z\sum_{p=1}^{3}\frac{\kappa C_p}{\alpha_p^2}\boldsymbol{\nabla}\{J_n(\alpha_p r)\cos n\theta\}. \tag{3.9}$$

The remaining independent solution needed for satisfaction of the four scalar boundary conditions (2.7) is provided by the complementary function (3.5) for $\boldsymbol{u}_h$ in which $\hat{F}$ is given by (3.6). Thus

$$\boldsymbol{u}_h = \boldsymbol{u}_h^{(1)} + \boldsymbol{u}_h^{(2)}, \tag{3.10}$$

where

$$\boldsymbol{u}_h^{(2)} = \mathrm{e}^{\gamma t}\sin\kappa z\, C_4\, \boldsymbol{g}\times\boldsymbol{\nabla}\{J_n(\alpha_4 r)\sin n\theta\} \tag{3.11}$$

and

$$\alpha_4^2 = -\kappa^2 - \gamma/\nu. \tag{3.12}$$

The four scalar boundary conditions specified in (2.7) yield four linear homogeneous equations for the constants C_1, C_2, C_3, C_4. The condition for these constants to be non-zero is that the fourth-order determinant formed from the coefficients of C_1, C_2, C_3, C_4 in the expressions for w, $\partial\rho'/\partial r$, and $\boldsymbol{u}_h$, as given by (3.7), (3.8) and (3.10) (with (3.9) and (3.11)) respectively at $r = a$, should be zero. This determinantal equation is the required eigenvalue relation giving $\gamma a^2/(\nu D)^{\frac{1}{2}}$ in terms of n, κa, ν/D and the Rayleigh number

$$R = \frac{ga^4}{D\nu\rho_0}\frac{\mathrm{d}\rho_1}{\mathrm{d}z}.$$

3.2. *Specific results for unstable modes*

The first work on the stability of stationary uniformly stratified fluid contained in a vertical circular cylinder appears to have been by Hales (1937), who was interested in the mechanism of geysers. He supposed, although later work has shown this to be incorrect, that the disturbance which grows at the smallest value of R would be axisymmetric. This corresponds to the choice $n = 0$ in the above relations, in which case the complementary function for $\boldsymbol{u}_h$ given by (3.11) is identically zero and the three scalar boundary conditions are matched by the three remaining fundamental solutions. Hales carried the calculation to completion and found values of R for a neutral disturbance ($\gamma = 0$) as a function of the vertical wavenumber κa. Later Yih (1959) confirmed and extended these calculations to a larger range of values of κa. The smallest value of R for which a neutral disturbance exists in this case $n = 0$ is 452, and occurs at $\kappa = 0$.

The fact established by Hales (and also later, analytically, by Yih 1959), that the critical axisymmetric disturbance to uniformly stratified fluid is a steady motion with straight vertical streamlines, seems likely to be true also for disturbances with other values of the azimuthal mode number n. Dr M. R. E. Proctor, who was kind enough to read this paper in draft form, told us he could prove that the neutral disturbance with the smallest Rayleigh number occurs at $\kappa = 0$ for any value of n, and at our invitation he gives his proof in the Appendix.

When $\kappa = 0$ there are only two roots of (3.4) for α^2, and for a neutral disturbance they are

$$\alpha_1^2 = R^{\frac{1}{2}}/a^2, \quad \alpha_2^2 = -R^{\frac{1}{2}}/a^2. \tag{3.13}$$

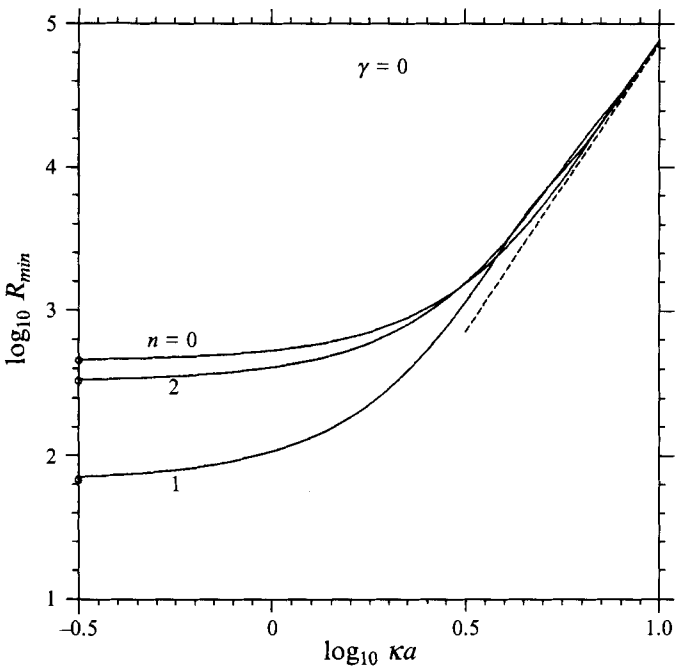

FIGURE 1. Rayleigh number $R(= (ga^4/D\nu\rho_0)(\mathrm{d}\rho_1/\mathrm{d}z))$ as a function of the vertical wavenumber κ for a neutral disturbance to stationary fluid with uniform density gradient in a vertical circular cylinder for each of the three azimuthal modes of lowest order. There is a sequence of neutral disturbances with different values of R for given n and κa, and only the smallest value of R is shown. The broken curve represents the asymptotic relation (3.18) which is independent of the presence of the cylindrical boundary.

The only two boundary conditions when $\kappa = 0$ are

$$w = 0, \quad \frac{\partial \rho'}{\partial r} = 0 \quad \text{at} \quad r = a,$$

and the condition that the two constants C_1 and C_2 in (3.7) and (3.8) should be non-zero when $\gamma = 0$ is then

$$J_n(R^{\frac{1}{4}}) J_n'(\mathrm{i}R^{\frac{1}{4}}) = \mathrm{i} J_n(\mathrm{i}R^{\frac{1}{4}}) J_n'(R^{\frac{1}{4}}). \tag{3.14}$$

Following Yih (1959), one may then find the smallest roots of this equation, for the first three azimuthal modes of a neutral disturbance with $\kappa = 0$:

$$\begin{array}{lccc} n = & 0 & 1 & 2 \\ R = & 452.0 & 67.96 & 328.9. \end{array}$$

At larger values of n the critical Rayleigh numbers are above that for $n = 2$. The mode $n = 1$ is clearly more effective in converting the potential energy in the undisturbed fluid to kinetic energy of the disturbance without too much dissipation or diffusion.

The first recognition of the importance of the mode $n = 1$ was by Taylor (1954), who stated in a review lecture about mass transport in tubes that his analysis of the instability of stratified fluid in a circular tube led to the conclusion that the fluid is stable for Rayleigh numbers less than 67.94. It seems likely that he hypothesized that the critical disturbance would be one for which $\kappa = 0$, and that he worked out the critical value of the Rayleigh number (perhaps for more than one value of n) in essentially the above way. He also confirmed the correctness of his theoretical result by an elegant measurement of the critical density gradient in a vertical circular tube.

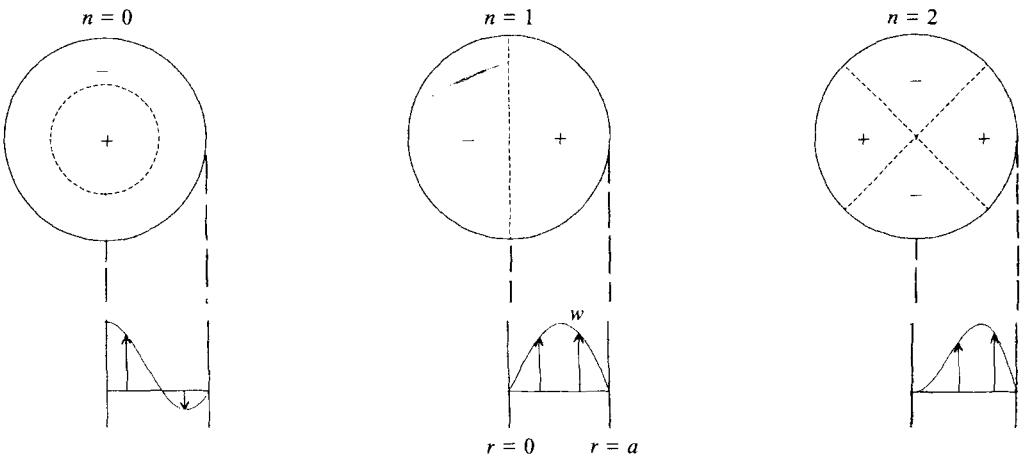

FIGURE 2. The distribution of vertical velocity in a circular cylinder for a neutral disturbance to uniformly stratified fluid with $\kappa = 0$ for the three azimuthal modes of lowest order. The density gradient in the undisturbed state is uniform. The signs + and − indicate regions of up and down flow respectively.

Instead of observing the maximum gradient for which the fluid remains stationary, as one normally would in the case of stratified fluid between horizontal parallel planes, he observed the minimum density gradient for which convective overturning exists. He connected the top of a tube full of clear water to a reservoir containing a dyed solution of salt, and waited until the convective motions in the tube had stopped. The observation consisted of measuring the length of tube into which the dye had penetrated, from which the critical density gradient could be found. Taylor noted that, once it has been confirmed that the critical density gradient is consistent with the above critical Rayleigh number, this is an effective method of measuring the diffusivity of the salt in solution.

In order to make the available results more complete we have calculated from the above analysis, with help from a computer in the handling of the fourth-order determinant, the smallest value of R for a neutral disturbance as a function of κa for the cases $n = 0$, $n = 1$ and $n = 2$, with results as shown in figure 1.† The expected minimum of each curve at $\kappa = 0$ is confirmed. Figure 2 gives some details of the velocity distribution at $\kappa = 0$ associated with each of these modes which we have calculated.

It is interesting to note that at large vertical wavenumbers the three curves corresponding to $n = 0, 1, 2$ intersect and that there exists a range of values of κa for which the axisymmetric mode is, in fact, the most unstable. Moreover, all three curves approach the same straight line asymptotically as $\kappa a \to \infty$ although not smoothly. These features are explicable if we recognize that at small vertical wavelengths the cylindrical walls have little influence on the planform of the flow. Aside from edge effects in regions near the circular boundary, the disturbance flow reduces to the cellular roll motion characterizing convection in an unbounded fluid, for which the neutral-stability relation takes the simple form

$$\frac{g}{D\nu\rho_0}\frac{\mathrm{d}\rho_1}{\mathrm{d}z} = \frac{(\kappa^2+\alpha^2)^3}{\alpha^2}, \tag{3.15}$$

† Yih gives explicitly the values of R at discrete values of κa for $n = 0$, and our values agree with his except that we find $R = 518$ at $\kappa a = 1$ and he gives $R = 528$.

where α is the horizontal wavenumber of a sinusoidal disturbance (BN1, §3). For any given value of κ, the most unstable (that is, having the smallest Rayleigh number) disturbance occurs at $\alpha = \kappa/\sqrt{2}$, whence

$$R_{min} = \frac{27}{4}(\kappa a)^4. \tag{3.16}$$

This is the equation of the dashed line in figure 1, and it describes the asymptotic behaviour of all the curves at large κa because at small vertical wavelengths all the azimuthal modes tend to unbounded-fluid roll motions and the distinction between them disappears. The wavy approach of the curves for $n = 1$ and $n = 2$ to the dashed line is probably a consequence of the fact that two-dimensional rolls are not exactly compatible with sectors of the circular cross-section.

The curves in figure 1 correspond to the neutral disturbances with the smallest Rayleigh number for each value of the azimuthal mode number n and for given κa. As would be expected of any eigenvalue problem posed on a bounded (here circular) domain, for each value of n and of κa there exist higher sub-modes with increasingly oscillatory radial dependences in addition to the most unstable sub-mode represented in figure 1. Although at small values of κa these sub-modes can be distinguished from each other by the number of zeros of w in the interval $0 < r < a$, at larger values of κa different sub-modes (corresponding to neutral disturbances for the same n and κa at different Rayleigh numbers) can have the same number of zeros. Thus, for example, at $n = 1$ and $\kappa a = 5$ the two smallest values of R at which a neutral disturbance exists are 6106 and 8986, and for both these neutral disturbances w has one zero in the interval $0 < r < a$.

Hitherto there have been no numerical results for values of the growth rate γ other than zero. We have therefore calculated from the determinantal eigenvalue equation values of $\gamma a^2/(\nu D)^{\frac{1}{2}}$ as a function of κa and R, the Prandtl number ν/D being put equal to unity for simplicity. (Note that the properties of a neutral disturbance are independent of ν/D.) Figure 3(*a*) shows the non-dimensional growth rate as a function of vertical wavenumber of the disturbance, for $n = 1$ and various small-to-moderate values of the Rayleigh number. The curves shown correspond to the fastest growing sub-mode for $n = 1$, hence the subscript *max* in γ_{max}. There is further illustration here of the fact that a disturbance for which $\kappa = 0$ is the most unstable.

In some circumstances values of γ at large values of R may be of practical interest, and so we extended the calculations to much larger values of R, including values for which effects of viscosity and diffusivity are likely to be negligible, the results being shown in figure 3(*b*). The variable on the ordinate scale here is

$$\frac{\gamma a^2}{(D\nu)^{\frac{1}{2}}} R^{-\frac{1}{2}} = \gamma \Big/ \left(\frac{g}{\rho_0}\frac{\mathrm{d}\rho_1}{\mathrm{d}z}\right)^{\frac{1}{2}}.$$

We saw in §2 that in the inviscid diffusionless limit γ is given by (2.12*b*), which in the case of a uniform density gradient and $W \propto \cos \kappa z$ reduces to

$$\gamma^2 = \frac{\alpha^2}{\alpha^2 + \kappa^2}\frac{g}{\rho_0}\frac{\mathrm{d}\rho_1}{\mathrm{d}z}. \tag{3.17}$$

Here α is given by (2.16*b*), namely

$$J_n'(\alpha a) = 0. \tag{3.18}$$

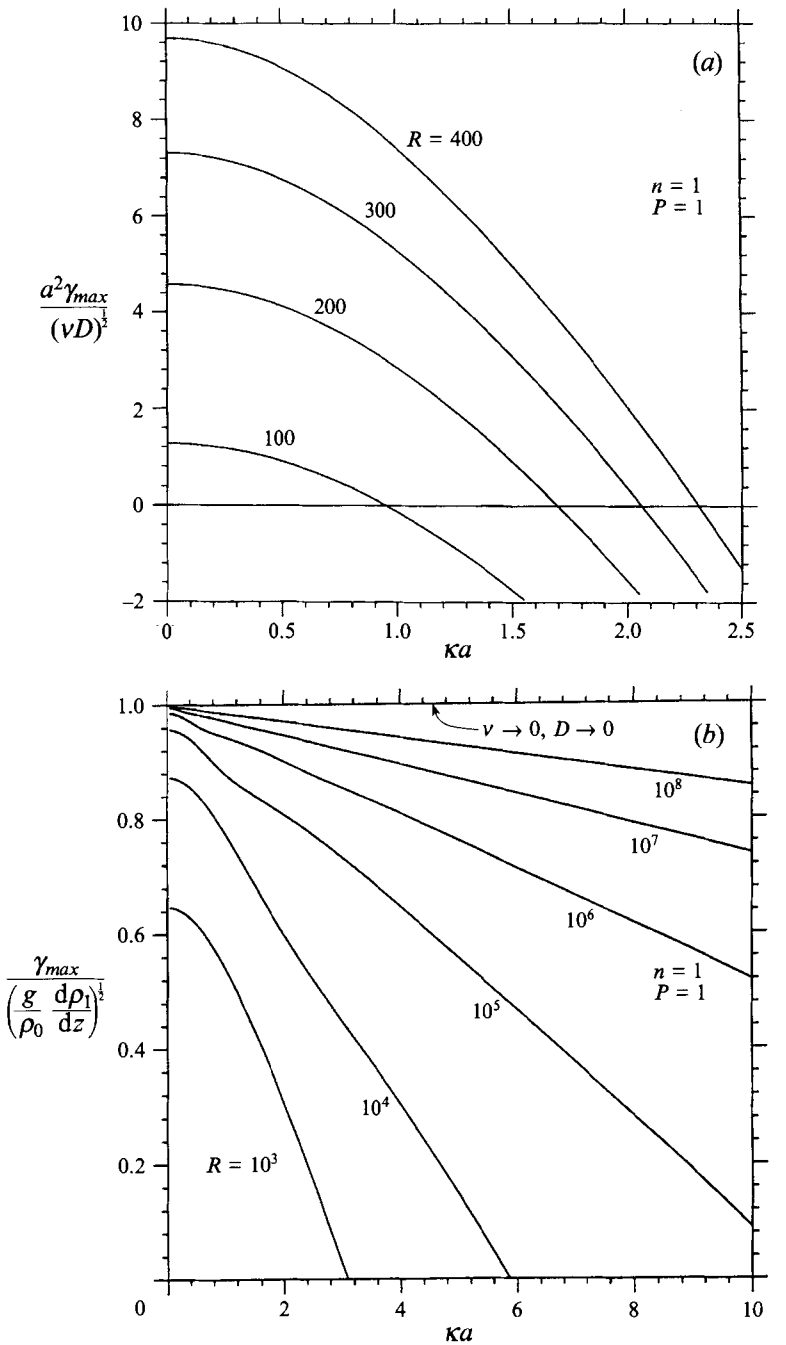

FIGURE 3. The largest of the values of the growth rate γ corresponding to a given wavenumber κ for a disturbance with azimuthal mode number $n = 1$ and a given value of the Rayleigh number. Undisturbed state: stationary fluid with uniform density gradient in a vertical circular cylinder; and $P = 1$. (*a*) Smaller values of R, and γ non-dimensionalized as $\gamma a^2/(\nu D)^{\frac{1}{2}}$; (*b*) larger values of R at which effects of viscosity and diffusion are likely to be small, and γ non-dimensionalized as $\gamma/((g/\rho_0)(d\rho_1/dz))^{\frac{1}{2}}$.

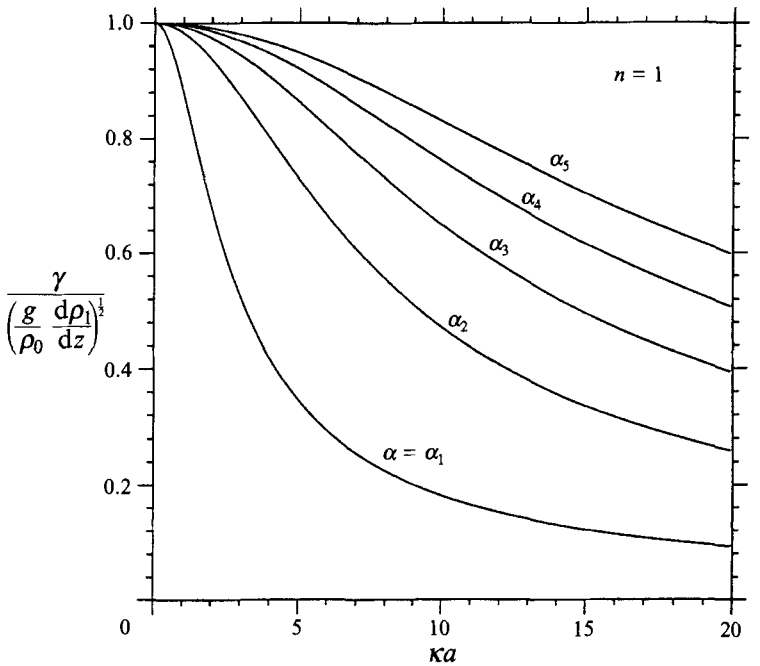

FIGURE 4. Growth rates of a disturbance in unbounded fluid with uniform density gradient in the inviscid diffusionless limit given by (3.17) and (3.18) for $n = 1$. $\alpha_1 a$ is the smallest root of (3.18), $\alpha_2 a$ is the next smallest, and so on.

Values of γ as a function of κa given by (3.17) and (3.18) are shown in figure 4 for $n = 1$ and sub-modes corresponding to the five smallest roots of (3.18) (e.g. $\alpha_1 a = 1.84$). These sub-modes can be ordered and counted. The largest growth rate for $n = 1$ and given κa is found by choosing an indefinitely large root of (3.18) for αa for which w exhibits a correspondingly large number of oscillations in the interval $0 < r < a$, so that in the inviscid diffusionless limit

$$\gamma_{max} = \left(\frac{g}{\rho_0}\frac{d\rho_1}{dz}\right)^{\frac{1}{2}} \tag{3.19}$$

for any value of κa. On the other hand, at small non-zero values of ν and D one would expect the fastest growing sub-mode to occur at a large but finite number of zeros of w in the interval $0 < r < a$, in which event γ would take a value less than that given by (3.19). The curves in figure 3(*b*) are consistent with these expectations.

The correspondence between the full analysis and the inviscid diffusionless limit for the azimuthal mode number $n = 1$ can be developed a little further, and proves to be interesting. In figure 5 we present calculations of γ as a function of κa at $R = 10^8$ for each of the 20 sub-modes corresponding to the 20 largest of the possible values of γ consistent with the chosen value of R. The uppermost of the 20 continuous curves shows the maximum value of γ as a function of κ, and so coincides with the uppermost curve in figure 3(*b*). The second highest curve shows the second largest of the possible values of γ, and so on. All the curves exhibit a striking step-like behaviour, and it is evident that collectively they describe a net composed of two intersecting families of curves. The down-steps trace out steep composite curves emanating from the upper left-hand corner of the figure. Each one of the steep curves made up of steps closely

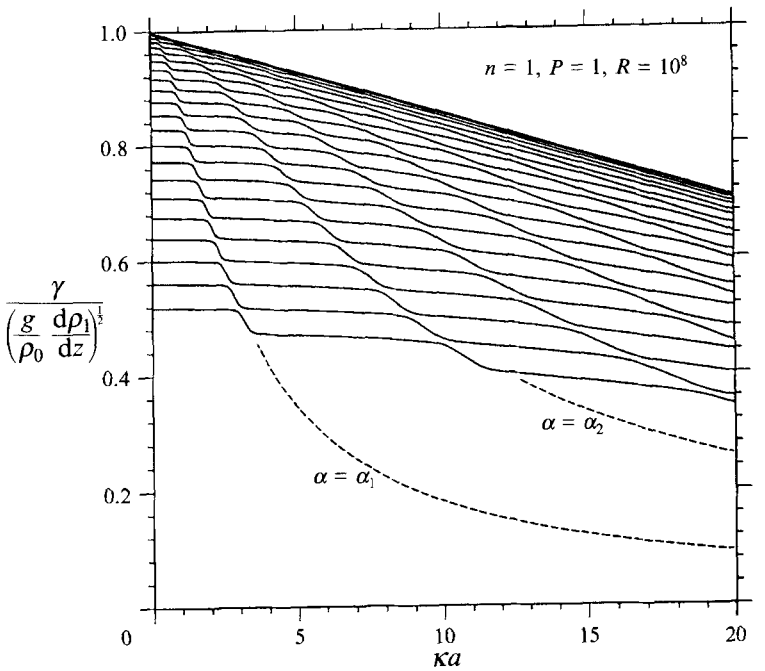

FIGURE 5. As for figure 3(*b*), except that $R = 10^8$ for all the curves. The uppermost of the 20 curves shows the maximum value of γ for a given value of κa, and so coincides with the uppermost curve in figure 3(*b*). The second highest curve shows the second largest of the possible values of γ, and so on. The interpretation of the net of two intersecting families of curves revealed by these 20 curves is given in the text. The broken lines, which are drawn only in the region outside the net, are the curves shown in figure 4 for the inviscid diffusionless limit.

approximates one of the curves in figure 4 representing the relation (3.17) between γ and κ for an inviscid sub-mode corresponding to one of the roots of (3.18) (with $n = 1$). Thus, at large Rayleigh number the curve for each sub-mode in the full calculation describes a portion of each of the curves representing the inviscid (infinite Rayleigh number) sub-modes.

The members of the second family of curves making up the net are nearly horizontal lines comprising nearly horizontal segments of the continuous curves, and their significance is as follows. The disturbance flow w corresponding to the fastest-growing sub-mode for $n = 1$ (the uppermost continuous curve in figure 5) has no zeros in the first nearly horizontal interval, one zero in the second such interval after the first down-step, two zeros in the third, etc.; w for the second viscous sub-mode has one zero in the first nearly horizontal interval, two in the second, etc.; w for the twentieth viscous sub-mode has nineteen zeros in the first nearly horizontal interval, twenty in the second, etc.; and so forth. Thus, the nearly horizontal lines obtained by jumping from one sub-mode to another are each characterized by a fixed number of zeros of w in the interval $0 < r < a$: no zeros for the top (and shortest) curve, one zero for the next highest, and so on.

4. A sinusoidal variation of the undisturbed density

The undisturbed fluid density is assumed here to have the steady form

$$\rho_0 + \rho_1(z) = \rho_0(1 + A \sin \kappa z). \tag{4.1}$$

In the absence of lateral boundaries this density distribution has been found to be highly unstable to disturbances with small horizontal wavenumbers, because a perturbation tilts the interleaved layers of heavy and light fluid and causes the heavy fluid to run down and collect in the troughs and the light fluid similarly to collect at the crests, thereby strengthening the original perturbation. Since the presence of a lateral boundary is generally incompatible geometrically with an indefinitely large horizontal wavelength of a disturbance, confinement within a vertical cylinder may materially affect the stability properties. Our purpose here is to quantify this effect for the case of a cylinder of circular cross-section.

For a cylinder radius a much larger than the vertical period $2\pi/\kappa$ (i.e. $a\kappa \gg 1$), it seems likely that the flow in the core region of the cross-section closely approximates the unbounded-fluid motion, and that the boundary merely puts a lower bound of order a^{-1} on the allowable horizontal wavenumbers. On the other hand, for a cylinder radius much smaller than the vertical period ($a\kappa \ll 1$), the disturbance flow must be driven by local instabilities in each half-period where the density stratification is statically unstable (cf. §3), with weak externally driven counter cells in the intervening statically stable intervals. These reasonable suppositions regarding the limiting cases will be tested by comparison with our numerical results.

4.1. *A numerical solution found from a finite-difference method*

For the sinusoidal base density profile (4.1) the dependence of the disturbance quantities upon the cylindrical coordinates r, θ, z is more complicated than in the constant-gradient case, where Fourier modes with respect to both θ and z were uncoupled and the radial structure was expressible as a superposition of Bessel functions. Disturbances with different azimuthal mode numbers n are here still independent so we shall again be at liberty to assume a single trigonometric angular dependence indexed by n. However, since $\mathrm{d}\rho_1/\mathrm{d}z$ is no longer constant, different Fourier modes of the disturbance with respect to z are coupled. Thus the r-dependent coefficients U_m, V_m, W_m, P_m, Q_m appearing in the general Fourier series expansions

$$\left.\begin{aligned} w &= \mathrm{e}^{\gamma t}(ga^2/\nu)\cos n\theta \sum_{m=0}^{\infty} W_m(r/a)\cos m\kappa z, \\ \boldsymbol{u}_h &= \mathrm{e}^{\gamma t}(ga^2/\nu) \sum_{m=0}^{\infty} \{\boldsymbol{i}_r \cos n\theta U_m(r/a) + \boldsymbol{i}_\theta \sin n\theta V_m(r/a)\} \sin m\kappa z, \\ p' &= \mathrm{e}^{\gamma t}\rho_0 ga \cos n\theta \sum_{m=0}^{\infty} P_m(r/a)\sin m\kappa z, \\ \rho' &= \mathrm{e}^{\gamma t}\rho_0 \cos n\theta \sum_{m=0}^{\infty} Q_m(r/a)\cos m\kappa z \end{aligned}\right\} \tag{4.2}$$

cannot be considered separately. As detailed below, coupling of the Fourier modes with respect to z is accounted for analytically in the manner of the three-term recurrence relation developed in BN1 for the unbounded-fluid case. Being unable to find an analytical representation of the r-dependence of the Fourier coefficients U_m, V_m, W_m, P_m, Q_m, we have resorted to finite-difference discretization.

Note that we have imposed here an *a priori* restriction to the synchronous disturbance for which w is even and periodic in z with period $2\pi/\kappa$, because this gives rise to the global tilting–sliding motion in the absence of lateral boundaries and was found in BN1 to be more unstable than any subharmonic disturbance.

Substitution of these Fourier series expansions into the governing equations (2.2), (2.3) and (2.5) leads to an infinite sequence ($m = 0, 1, 2, \ldots$) of systems of five coupled ordinary differential equations having the form

$$\left.\begin{aligned}
\{\mathscr{L}-(n^2+1)/\xi^2-(m\kappa a)^2-(\gamma a^2/\nu)\}\,U_m(\xi)-(2n/\xi^2)\,V_m(\xi)-\mathrm{d}P_m/\mathrm{d}\xi &= 0,\\
\{\mathscr{L}-(n^2+1)/\xi^2-(m\kappa a)^2-(\gamma a^2/\nu)\}\,V_m(\xi)-(2n/\xi^2)\,U_m(\xi)+(n/\xi)\,P_m(\xi) &= 0,\\
\{\mathscr{L}-n^2/\xi^2-(m\kappa a)^2-(\gamma a^2/\nu)\}\,W_m(\xi)-m\kappa a P_m(\xi)-Q_m(\xi) &= 0,\\
\{\mathscr{L}-n^2/\xi^2-(m\kappa a)^2\}\,P_m(\xi)-m\kappa a Q_m(\xi) &= 0,
\end{aligned}\right\} \tag{4.3}$$

$$\{\mathscr{L}-n^2/\xi^2-(m\kappa a)^2-P(\gamma a^2/\nu)\}\,Q_m(\xi) = \tfrac{1}{2}R\begin{cases} W_1(\xi), & m=0\\ 2W_0(\xi)+W_2(\xi), & m=1\\ W_{m-1}(\xi)+W_{m+1}(\xi), & m\geqslant 2,\end{cases}$$

in which $\xi = r/a$ is a dimensionless radial coordinate, $\mathscr{L}$ represents the differential operator $\xi^{-1}(\mathrm{d}/\mathrm{d}\xi)(\xi\,\mathrm{d}/\mathrm{d}\xi)$, R is the Rayleigh number $gA\kappa a^4/\nu D$ and $P = \nu/D$ is the Prandtl number. The right-hand side of the last of these equations couples the system (4.3) for each m with the corresponding systems for $m-1$ and $m+1$. The appropriate boundary conditions at the cylindrical wall are

$$U_m = V_m = W_m = 0, \quad \mathrm{d}U_m/\mathrm{d}\xi = \mathrm{d}Q_m/\mathrm{d}\xi = 0 \quad \text{at} \quad \xi = 1,$$

the fourth equation deriving from fluid incompressibility.

For numerical purposes, the usual weak requirement of non-singularity at the axis ($\xi = 0$) must be expressed in a concrete form. Considerations of symmetry indicate that the appropriate conditions depend upon the mode number n as follows:

$$\begin{aligned}
n = 0\text{:}\quad & U_m = V_m = 0, \quad \mathrm{d}W_m/\mathrm{d}\xi = \mathrm{d}P_m/\mathrm{d}\xi = \mathrm{d}Q_m/\mathrm{d}\xi = 0 \quad \text{at} \quad \xi = 0,\\
n \geqslant 1\text{:}\quad & W_m = P_m = Q_m = 0, \quad \mathrm{d}U_m/\mathrm{d}\xi = \mathrm{d}V_m/\mathrm{d}\xi = 0 \quad \text{at} \quad \xi = 0.
\end{aligned}$$

As in the unbounded-fluid case, an approximate solution for the disturbance quantities can be obtained by truncation of the Fourier series in z, i.e. by assuming that

$$U_m(\xi) = V_m(\xi) = W_m(\xi) = P_m(\xi) = Q_m(\xi) \equiv 0 \quad \text{for} \quad m > M, \tag{4.4}$$

with M a sufficiently large integer. The resulting finite system of equations (4.3) has been discretized using five-point central-difference formulae accurate to within error terms of order h^4 in the subdivision $h = 1/N$ of the unit interval $0 \leqslant \xi \leqslant 1$, together with forward and backward formulae at the ends of the interval. This discretization leads to the grand $\mathscr{N}\times\mathscr{N}$ generalized matrix eigenvalue equation

$$\begin{pmatrix} \boldsymbol{A}_0 & & & \\ & \boldsymbol{A}_1 & & \\ & & \boldsymbol{A}_2 & \\ & & & \ddots \end{pmatrix}\begin{pmatrix} X_0\\ X_1\\ X_2\\ \vdots \end{pmatrix} = \tfrac{1}{2}R\begin{pmatrix} & \boldsymbol{B} & & \\ 2\boldsymbol{B} & & \boldsymbol{B} & \\ & \boldsymbol{B} & & \boldsymbol{B} \\ & & \cdots & \end{pmatrix}\begin{pmatrix} X_0\\ X_1\\ X_2\\ \vdots \end{pmatrix}, \tag{4.5}$$

with $\mathscr{N} = 5(M+1)(N+1)$. Here, the sub-matrix $\boldsymbol{A}_m$ represents the discretization of the left-hand sides of (4.3) for given m and $\boldsymbol{B}$ is very sparse because W_m alone appears in the right-hand sides of the equations in (4.3). Equation (4.5) is directly analogous to the corresponding three-term recurrence relation (5.14) in BN1 applicable to the unbounded-fluid case. Eigenvalues of (4.5) are determined numerically with the help of EISPACK subroutines (Dongarra & Moler 1984).

It is worth noting that the eigenvalue relation

$$\boldsymbol{A}_1 X_1 = R\boldsymbol{B}X_1 \tag{4.6}$$

Number of subdivisions	Rayleigh number, R
10	134.76076
20	134.77836
40	134.77966
Exact value by method of §3	134.77964

TABLE 1. Values of the Rayleigh number computed by the finite-difference method for the case of constant density gradient with $n = 1$, $\kappa a = 1$, $\gamma a^2/(\nu D)^{\frac{1}{2}} = 1$, $P = 1$

describes the constant-gradient case discussed in §3. We have checked our finite-difference scheme by applying it to the case of uniform density gradient and comparing the results with those obtained in §3 by the more analytical method. As an example of the accuracy of the computations, table 1 demonstrates the rapid convergence of the smallest eigenvalue of (4.6) to the Rayleigh number computed using the method of §3 for specific parameter values.

We saw in §3 that in the case of a uniform density gradient $n = 1$ is the most unstable azimuthal mode. We shall suppose, with no more than intuitive justification, that this is also true for a sinusoidal density profile, and shall therefore confine our numerical calculations here to the case $n = 1$.

In discussion of values of κa ranging from very small to very large, it is convenient to introduce two Rayleigh numbers, namely

$$R_a = \frac{gA\kappa a^4}{\nu D} \quad \text{and} \quad R_\kappa = \frac{gA}{\nu D\kappa^3}.$$

Both are based on the maximum undisturbed density gradient $\rho_0 A\kappa$, but they differ in the choice of characteristic lengths, a and κ^{-1} respectively. The first corresponds to the Rayleigh number defined in §3, and is appropriate for the range $\kappa a \ll 1$, in which the lateral boundary exerts a dominant influence on the flow. The second was introduced for the unbounded-fluid case in BN1 and is natural for the opposite range $\kappa a \gg 1$, because fluid motion driven by the vertical stratification is affected in only a subsidiary way by the boundary. Figure 6 shows the calculated dependences of these Rayleigh numbers upon the dimensionless vertical wavenumber κa for neutral and non-neutral disturbances, and figure 7 displays calculated streamlines in the plane $\theta = 0$ for neutral disturbances at $\kappa a = 2$; and all these results apply when $n = 1$ and $P = 1$.

4.2. *The limiting cases* $\kappa a \to 0$ *and* $\kappa a \to \infty$

As $\kappa a \to 0$ the Rayleigh number R_a approaches the value for a zero-wavenumber disturbance in a cylinder with constant gradient equal to $\rho_0 A\kappa$ (i.e. the maximum value of $\rho_0 A\kappa \cos \kappa z$), represented by dashed lines in figure 6(*a*). Near $z = 2\pi p/\kappa$, where p is an integer, the undisturbed density gradient appears constant on the scale of the cylinder radius a and equal to $\rho_0 A\kappa$, so it is understandable that overturning sets in locally exactly as found in §3. Since there exist intervening layers of stably stratified fluid, the flow must close in rolls instead of being completely uniform in z (with weak externally driven rolls in the stably stratified intervals) but the vertical extent of the rolls is much larger than a, so the flow certainly approximates unidirectional motion near $z = 2\pi p/\kappa$.

Further insight into the limit $\kappa a \to 0$ can be obtained by studying the set of coupled systems (4.3) with $m = 0, 1, 2, \ldots$, or its discretized version (4.5). As $\kappa a \to 0$, the Fourier mode number m formally disappears from the governing equations, because m

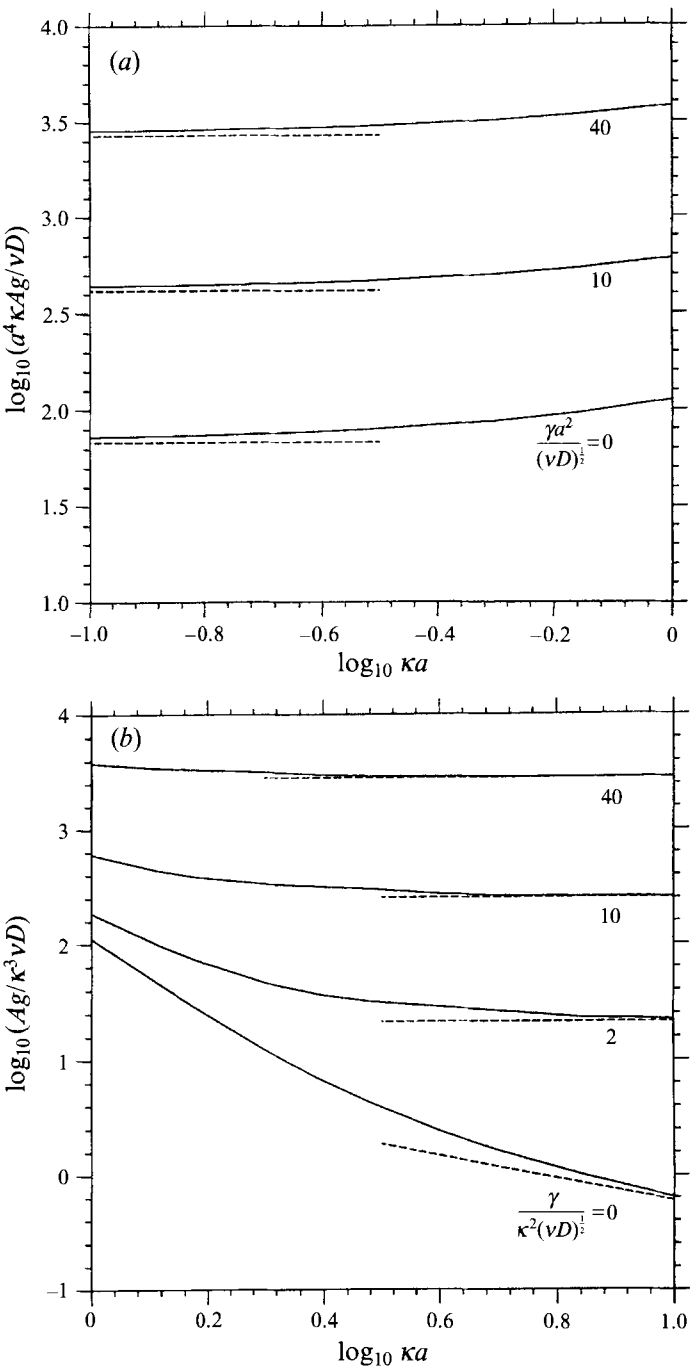

FIGURE 6. Results of a numerical finite-difference calculation for the Rayleigh number corresponding to a given growth rate of a disturbance to fluid in a vertical circular cylinder with sinusoidal density variation; $n = 1$ and $P = 1$ for all curves. (*a*) Rayleigh number $R_a = a^4\kappa Ag/\nu D$ as a function of κa for given values of $\gamma a^2/(\nu D)^{\frac{1}{2}}$; (*b*) $R_\kappa = Ag/\kappa^3\nu D$ as a function of κa for given $\gamma/\kappa^2(\nu D)^{\frac{1}{2}}$. The asymptotic straight lines at $\kappa a \ll 1$ and $\kappa a \gg 1$ are explained in the text.

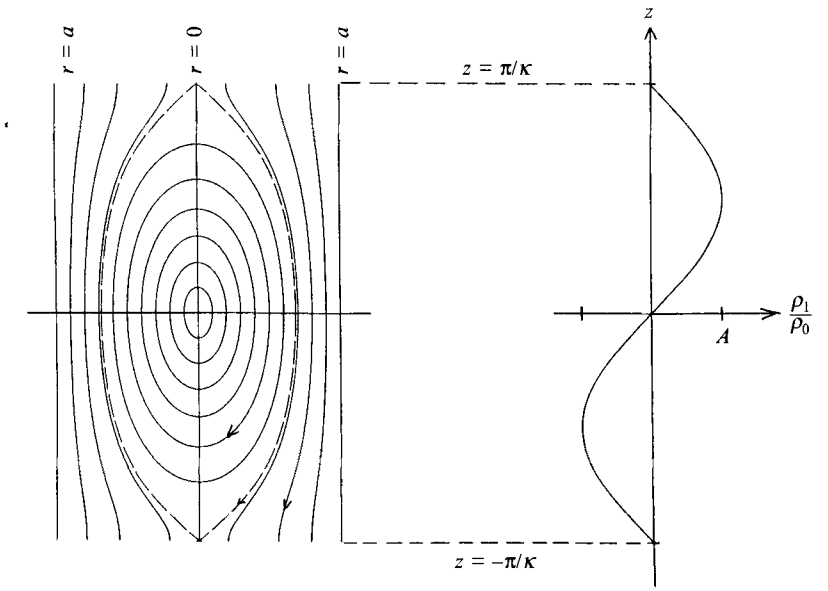

FIGURE 7. Streamlines of a neutral disturbance in the plane $\theta = 0$ through the axis of a circular cylinder; $n = 1$, $\rho_1 = \rho_0 A \sin \kappa z$, $\kappa a = 2.0$.

invariably appears in the form of the combination $m\kappa a$. Thus, one might suspect that the intrinsic radial dependence of all the Fourier coefficients becomes independent of m, i.e.

$$\{U_m(\xi), V_m(\xi), W_m(\xi), P_m(\xi), Q_m(\xi)\} = C_m\{U(\xi), V(\xi), W(\xi), P(\xi), Q(\xi)\},$$

where U, V, W, P, Q represent universal functions of ξ and the $C_m (m = 0, 1, 2, \ldots)$ are constants, as yet undetermined. Equivalently, in discretized form

$$\boldsymbol{X}_m = C_m \boldsymbol{X}. \tag{4.7}$$

Substitution of (4.7) into (4.5) leads precisely to the system (4.6) with $\kappa a = 0$ for the eigenvalue R_a and the functions U, V, W, P, Q comprising the eigenvector $\boldsymbol{X}$, together with the recursion relation

$$\left.\begin{aligned} C_0 &= \tfrac{1}{2}C_1, \quad C_1 = C_0 + \tfrac{1}{2}C_2, \\ C_m &= \tfrac{1}{2}(C_{m-1} + C_{m+1}), \quad m \geqslant 2. \end{aligned}\right\} \tag{4.8}$$

Thus, as $\kappa a \to 0$, the eigenvalue R_a approaches the zero-wavenumber value for the case of a constant density gradient of magnitude $\rho_0 A\kappa$. The solution of (4.8) is

$$C_m = 2C_0 \,\forall\, m \geqslant 1. \tag{4.9}$$

These Fourier coefficients describe the periodic delta distribution

$$\frac{2\pi C_0}{\kappa} \sum_{p=-\infty}^{\infty} \delta\left(z - \frac{2\pi p}{\kappa}\right). \tag{4.10}$$

Formal delta dependence implies that the z-interval where the flow has appreciable strength is small compared with the vertical period $2\pi/\kappa$. At the same time, we know this interval to be large compared with a. Thus, appreciable flow strength is confined to a region intermediate in scale between a and κ^{-1}. We have checked that the

numerically computed Fourier coefficients $U_m(\xi)$, $V_m(\xi)$, $W_m(\xi)$, $P_m(\xi)$, $Q_m(\xi)$ seem to conform to (4.7) over an increasing range of m as $\kappa a \to 0$. Indeed the preceding considerations explain the observed slow convergence of the numerical scheme with increasing M in the limit $\kappa a \to 0$.

The fact that the value of R_a for given γ shown in figure 6(*a*) is the same, when $\kappa a \ll 1$, as for fluid in a vertical tube with a uniform density gradient of magnitude $\rho_0 \kappa A$ does not involve the sinusoidal form of $\mathrm{d}\rho_1/\mathrm{d}z$; all that is relevant is the maximum value of $\mathrm{d}\rho_1/\mathrm{d}z$. It follows then that the same result holds for ρ_1 equal to any periodic function of z with large wavelength which is continuous in z with bounded slope, whence the largest value of the density gradient for a neutral disturbance to fluid in a vertical tube for which ρ_1 is periodic in z with wavelength large compared with a is given by

$$\frac{ga^4}{\rho_0 \nu D}\left(\frac{\mathrm{d}\rho_1}{\mathrm{d}z}\right)_{max} = 67.96.$$

In the limit $\kappa a \to \infty$, the Rayleigh number R_κ for a neutral disturbance evidently becomes inversely proportional to κa. The empirical asymptote to the $\gamma = 0$ curve which has been drawn as a broken line in figure 6(*b*) is given by $R_\kappa = 5.924(\kappa a)^{-1}$, which is compatible quantitatively with the unbounded-fluid scaling law

$$R_\kappa \sim \sqrt{2}\alpha/\kappa \quad \text{when} \quad \gamma = 0 \tag{4.11}$$

derived in BN1 if one defines α such that $\pi/\alpha = 0.75a$. This fits well with our expectation that the main influence of the walls upon the unbounded-fluid tilting–sliding mechanism is simply the selection of a dominant horizontal wavenumber α such that downflow occurs in one half of the cylinder cross-section and upflow in the other. Since a circular boundary is incompatible geometrically with the two-dimensional unbounded-fluid motion, one cannot expect the horizontal half-period π/α to equal exactly the cylinder radius a, but the numerical correspondence is close. Calculated streamlines in figure 7 for $\kappa a = 2$ bear a striking resemblance to streamlines for the unbounded-fluid case (see figure 5, BN1), indicating the unimportance of the cylindrical walls. In particular, they again exhibit a central eye-shaped region of closed-roll motion separated from adjacent regions of upflow and downflow by dividing streamlines.

For fixed *non-zero* γ, the most unstable unbounded-fluid disturbance (i.e. the disturbance having the smallest Rayleigh number compatible with the given γ) was found in BN1 to occur at a finite horizontal wavenumber α, not $\alpha = 0$. For example, for $\gamma/\kappa^2(\nu D)^{\frac{1}{2}} = 10$ the minimum R_κ is 253 and occurs at $\alpha/\kappa = 1.18$. The unbounded system itself selects a dominant wavenumber α of order κ, so in the limit as $\kappa a \to \infty$ the walls play no role (aside from causing edge effects very near the boundaries) in determining the Rayleigh number in the cylinder. The approach of the calculated curve for $\gamma/\kappa^2(\nu D)^{\frac{1}{2}} = 10$ to the asymptotic value $R_\kappa = 253$ in figure 6(*b*) represents confirmation of the numerical calculations.

4.3. *Inviscid diffusionless fluid*

It was noted in §2 that simple supplementary results applicable to cases in which $\gamma l^2/\nu$ and $\gamma l^2/D$ are large may be obtained by putting $\nu = 0$ and $D = 0$ in the governing equations. These equations reduce to (2.12), and the allowable values of α for fluid contained in a vertical circular cylinder were seen to be given by the roots of

$$J_n'(\alpha a) = 0. \tag{4.12}$$

The growth rate γ is then to be found as an eigenvalue of (2.12*b*) after substitution of the appropriate expression for $\mathrm{d}\rho_1/\mathrm{d}z$.

In the present case ρ_1 is given by (4.1) and the equation for $W(z)$ becomes

$$\frac{\mathrm{d}^2 W}{\mathrm{d}z^2}+\alpha^2 W\left(\frac{g\kappa A}{\gamma^2}\cos\kappa z-1\right)=0. \tag{4.13}$$

It was found in §5 of BN1 that a remarkably accurate solution of the more general form of (4.13) in which ν and D are not equated to zero can be obtained by writing W as a Fourier series with period $2\pi/\kappa$ and truncating the series after a few terms. That procedure gave the algebraic equation (5.17) in BN1 for γ in the case of the most unstable mode, and the form taken by that equation when $\nu = 0$ and $D = 0$ is

$$\gamma^2 = \frac{\alpha\kappa g A}{\sqrt{2}(\kappa^2+\alpha^2)^{\frac{1}{2}}}. \tag{4.14}$$

Note that in the case of unbounded fluid the analogous formula is (7.3) in BN1, which coincides with (4.14) when $\kappa/\alpha \to \infty$, as expected. Note also that in (7.3) in BN1 α is an arbitrary horizontal wavenumber of a Fourier component of the disturbance, whereas here α must satisfy (4.12). Comparison may also be made with the formula (3.17) for γ in the case of inviscid diffusionless fluid in a circular cylinder with a uniform undisturbed density gradient. Except when $\alpha/\kappa \ll 1$ the two formulae, namely (3.17) and (4.14), give values of γ of the same order of magnitude if the uniform density gradient is equated with a representative magnitude of the sinusoidal density gradient; and when $\alpha/\kappa \ll 1$ the value of γ given by (4.14) for the sinusoidal gradient is an order of magnitude larger than that given by (3.17) for the uniform gradient because the tilting–sliding mechanism operates in the former case but not in the latter.

5. Uniform density outside a thin central layer

It was shown in our previous paper (BN1, §6) that there are connections between the stability properties of unbounded fluid with a sinusoidal vertical density profile and those for fluid whose density in the undisturbed state is uniform except in a single horizontal central layer. In particular, the disturbance that is unstable at the smallest value of the Rayleigh number for given (large) horizontal wavelength involves a characteristic tilting and sliding of the thin layers of uniform density in both cases. Here we consider the effect of the presence of a vertical cylindrical boundary on the stability of fluid whose density $\rho_0+\rho_1$ has the uniform value ρ_0 everywhere except in a central layer whose thickness l is small compared with the linear dimension a of the cylinder cross-section. Typical forms of the function $\rho_1(z)$ for consideration are those designated in BN1 as type 2 or 2′ (with a single extremum, like a Gaussian function) and type 3 or 3′ (with two extrema and zero total excess mass, like the derivative of a Gaussian function). It may be expected that the presence of the cylindrical boundary excludes disturbances with horizontal lengthscales larger than a and that this leads to a non-zero minimum Rayleigh number for neutrality, as was found in the previous section for a sinusoidal density profile.

The general stability analysis of viscous fluid with variable density only in a central layer appears to be difficult when the effect of a rigid cylindrical boundary is included. Our analysis in this section will perforce be largely concerned with the simpler case of fluid which is effectively inviscid and diffusionless. In these circumstances there are no neutral disturbances, and degrees of instability under different conditions will be

indicated by relative values of the growth rate γ. At the end of the section we return to the effects of viscosity and diffusion in order to be able to estimate the maximum growth rates of a disturbance.

5.1. *Asymptotic analysis for the case* $\alpha l \ll 1$, $\nu = 0$, $D = 0$

We saw in §2 that some of the allowed values of the generalized horizontal wavenumber α in this case are such that α^{-1} is comparable with the linear dimensions of the cylinder cross-section; there is no contradiction therefore in supposing that

$$\alpha l \ll 1,$$

where l is a measure of the thickness of the central layer. This assumption makes possible a simple local analysis of the tilting–sliding mechanism and an approximate derivation of the rate of growth of the disturbance.

Outside the central layer the inviscid-fluid motion is irrotational, and with the requirement that $W \to 0$ as $z \to \pm\infty$ we see that $W(z)$ varies, according to (2.12*b*), as $\exp(\mp\alpha z)$. The vertical velocity component w is approximately continuous across the thin approximately horizontal layer, with value W_1 say, and so

$$W(z) = \begin{cases} W_1 \mathrm{e}^{-\alpha z} & \text{for} \quad z > 0 \\ W_1 \mathrm{e}^{\alpha z} & \text{for} \quad z < 0. \end{cases} \tag{5.1}$$

Now consider the motion within the thin central layer. The mechanical process that generates the growing disturbance is the sliding of layers of heavy or light fluid tilted slightly from the horizontal. The local vertical displacement of a material lamina of fluid of density $\rho_0 + \rho_1$, $\eta(\boldsymbol{x}_h)$ say, increases at the rate

$$\partial\eta/\partial t = (w)_{z=0} = \mathrm{e}^{\gamma t} W_1 F(\boldsymbol{x}_h),$$

and the acceleration of the lamina due to gravity down (or up, if $\rho_1 < 0$) a slope of small angle $\nabla\eta$ to the horizontal is

$$\frac{\partial \boldsymbol{u}_h}{\partial t} = -\frac{g\rho_1}{\rho_0}\nabla\eta, \tag{5.2}$$

whence

$$\boldsymbol{u}_h = -\mathrm{e}^{\gamma t} W_1 \frac{g\rho_1}{\gamma^2\rho_0}\nabla F. \tag{5.3}$$

The corresponding contribution to $\partial w/\partial z$ is

$$\frac{\partial w}{\partial z} = -\nabla\cdot\boldsymbol{u}_h = -\mathrm{e}^{\gamma t}\alpha^2 W_1 \frac{g\rho_1}{\gamma^2\rho_0} F,$$

that is,

$$\frac{\mathrm{d}W}{\mathrm{d}z} = -\alpha^2 W_1 \frac{g\rho_1}{\gamma^2\rho_0} \tag{5.4}$$

within the central layer.

We now integrate the governing equation for $W(z)$ in (2.12), with neglect of the second term within brackets (to be justified in a moment), to obtain

$$\int_L \frac{\mathrm{d}^2 W}{\mathrm{d}z^2}\mathrm{d}z = -\frac{\alpha^2 g}{\gamma^2\rho_0}\int_L W\frac{\mathrm{d}\rho_1}{\mathrm{d}z}\mathrm{d}z,$$

whence

$$\left[\frac{\mathrm{d}W}{\mathrm{d}z}\right]_L = \frac{\alpha^2 g}{\gamma^2\rho_0}\int_L \frac{\mathrm{d}W}{\mathrm{d}z}\rho_1\,\mathrm{d}z, \tag{5.5}$$

where L indicates integration across the layer, with $\rho_1 = 0$ at the two terminal points, and the square brackets denote a jump between those two termini. The jump in $\mathrm{d}W/\mathrm{d}z$ is determined by the two outer irrotational flow fields (5.1) and is $-2\alpha W_1$. Hence on substituting the value of $\mathrm{d}W/\mathrm{d}z$ given by (5.4) in the integral in (5.5) at points within the layer we find

$$\gamma^4 \approx \tfrac{1}{2}\alpha^3 g^2 \int_{-\infty}^{\infty} \frac{\rho_1^2}{\rho_0^2}\,\mathrm{d}z, \tag{5.6}$$

in which, it will be recalled from §2, the value of α is given by $J_n'(\alpha a) = 0$. With this expression for γ the order of magnitude of $(g/\gamma^2\rho_0)(\mathrm{d}\rho_1/\mathrm{d}z)$ is $(\alpha l)^{-\frac{3}{2}}$, showing that the second term within brackets in (2.12*b*) for $W(z)$ is indeed negligible when $\alpha l \ll 1$.

This is a suitable point at which to correct an error in BN1 which has some intrinsic interest. Section 7.2 in that paper described an energy argument giving the growth rate of a disturbance to unbounded inviscid diffusionless fluid whose density differs from ρ_0 only in a central horizontal layer. The disturbance was assumed to vary sinusoidally with respect to a horizontal position coordinate, with wavenumber α. The result (5.6) should coincide with that found from the energy argument in BN1, but in fact the value of γ^4 found there is larger by a factor 2. The reason for this discrepancy eluded us until we realized that the lateral sliding of a lamina of density $\rho_0 + \rho_1$ causes a local vertical volume flux $\boldsymbol{u}_h \cdot \boldsymbol{\nabla}\eta$, of which the mean over the cylinder cross-section S is approximately

$$\begin{aligned} \langle \boldsymbol{u}_h \cdot \boldsymbol{\nabla}\eta \rangle &= -\mathrm{e}^{2\gamma t} W_1^2 \frac{g\rho_1}{\gamma^3 \rho_0} \frac{1}{S} \int (\boldsymbol{\nabla} F)^2 \,\mathrm{d}S, \\ &= -\tfrac{1}{2}\mathrm{e}^{2\gamma t} W_1^2 \frac{\alpha^2 g \rho_1}{\gamma^3 \rho_0} \end{aligned} \tag{5.7}$$

on use of the boundary condition (2.15) and the normalizing relation (2.13). In reality the mean vertical volume flux at the central layer must be zero in view of the supposed presence of an impermeable bottom to the container which provides the force (transmitted by pressure in the fluid) that balances the gravitational force on the layer. The presence of the spurious mean vertical volume flux has no consequences for the above set of relations between first-order disturbance quantities, but a second-order mean volume flux does play a part in the energy argument and makes a contribution

$$\int_L \langle \boldsymbol{u}_h \cdot \boldsymbol{\nabla}\eta \rangle g\rho_1 \,\mathrm{d}z = -\tfrac{1}{2}\mathrm{e}^{2\gamma t}\rho_0 W_1^2 \frac{\alpha^2 g^2}{\gamma^3} \int_{-\infty}^{\infty} \frac{\rho_1^2}{\rho_0^2}\,\mathrm{d}z \tag{5.8}$$

to the rate of change of potential energy per unit horizontal area of the central layer. In order to correct the energy argument, therefore, the expression (5.8) must be deducted from the expression for $\mathrm{d}P/\mathrm{d}t$ given in (7.13) of BN1; and the effect of this is to require the insertion of the factor $\frac{1}{2}$ on the right-hand sides of the relations (7.13), (7.14) and (7.15) in BN1, thereby reconciling the result of the energy argument with our present result (5.6). The way in which the existence of the container bottom influences the energy argument is mathematically reminiscent of the effect of the constraint of constant liquid volume on the energy balance for a perturbed cylindrical column of liquid made unstable by the effect of surface tension (Chandrasekhar 1961, §111).

We see from expression (5.6) for the growth rate that the effect of the vertical distribution of density in the undisturbed fluid is represented by the parameter

$$I = \int_{-\infty}^{\infty} \frac{\rho_1^2}{\rho_0^2}\,\mathrm{d}z, \tag{5.9}$$

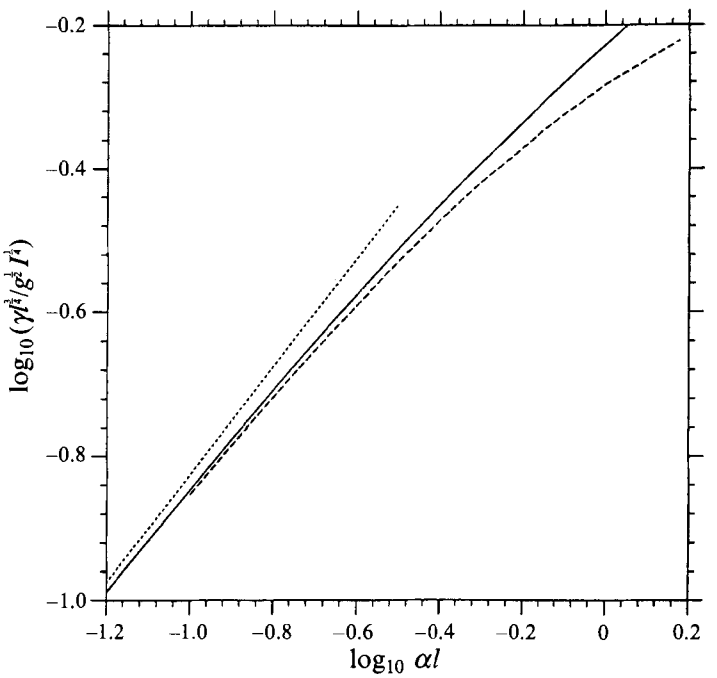

FIGURE 8. The growth rate of a disturbance to fluid whose density differs from ρ_1 only in a central layer of thickness l when $\nu = 0$ and $D = 0$. The dotted curve shows the result (5.6) of asymptotic analysis for $\alpha l \ll 1$; the dashed curve represents a finite-difference solution of the governing equation for $W(z)$ for the Gaussian density profile (5.10); and the continuous curve represents an exact solution of the governing equation for the piecewise-constant density profile (5.12). The horizontal wavenumber α is determined by satisfaction of the condition (2.16*b*) of no flux of fluid across the cylinder boundary.

as may be understood from the fact that each lamina within the central layer slides independently of its neighbours (in inviscid diffusionless fluid) with a velocity proportional to ρ_1/ρ_0. The sign of ρ_1/ρ_0 is immaterial, and in particular the qualitative difference between zero and non-zero values of the total excess mass in the central layer that we found at small Rayleigh numbers (BN1, §6) does not exist. Note also that the maximum value of the density gradient in the central layer has no special relevance. In the particular case of the Gaussian density profile given by

$$\frac{\rho_1}{\rho_0} = \frac{A}{\pi^{\frac{1}{2}}} e^{-z^2/l^2}, \quad I = \frac{A^2 l}{(2\pi)^{\frac{1}{2}}}, \tag{5.10}$$

the expression (5.6) for the growth rate becomes

$$\gamma^4 = 2^{-\frac{3}{2}}\pi^{-\frac{1}{2}}\alpha^3 g^2 l A^2. \tag{5.11}$$

5.2. *More accurate results for particular density profiles when* $\nu = 0$, $D = 0$

In order to be able to estimate the magnitude of the error in our asymptotic analysis, which is applicable for $\alpha l \ll 1$, we have found a numerical solution of (2.12*b*) for $W(z)$ by finite-difference methods for the case of a Gaussian density profile (5.10). The resulting relation between γ and αl is compared in figure 8 with the asymptotic relation (5.6), with γ being made non-dimensional by use of the factor I for both curves so that the curve representing the asymptotic relation is applicable to any density profile. At $\alpha l = 0.1$ the value of γ given by the asymptotic formula is only 6% too large. An

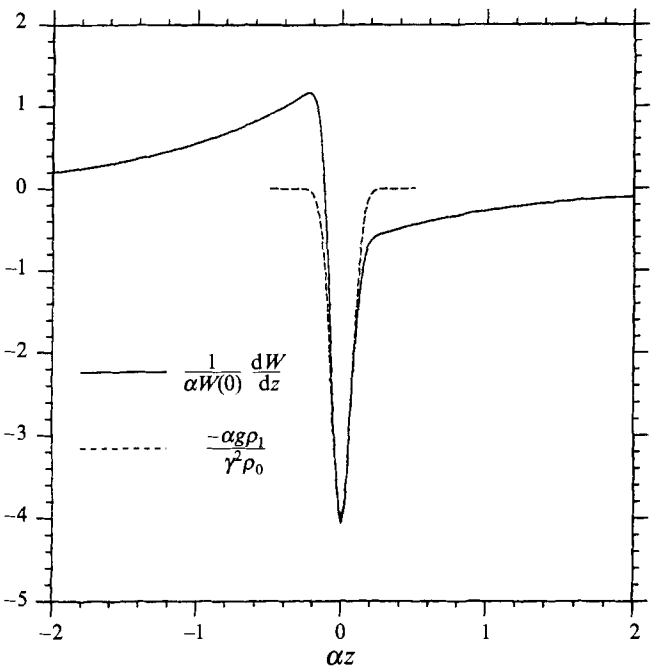

FIGURE 9. A numerical check on the formula (5.4) relating the rapid variations of dW/dz and ρ_1/ρ_0 with z within the thin central layer. The undisturbed density ρ_1 has the Gaussian form (5.10), and $\alpha l = 0.1$.

interesting by-product of the numerical solution for the case of a Gaussian density profile is the continuous curve in figure 9 representing values of dW/dz (in non-dimensional form) as a function of αz when $\alpha l = 0.1$. According to the asymptotic analysis, the rapid variation of dW/dz within the layer is identical with that of ρ_1/ρ_0, and the comparison of the computed values of dW/dz with those given by (5.4) (together with (5.10) and (5.11)) shows that this is indeed so.

In §6.2 of BN1 we described an exact solution for a disturbance to unbounded fluid whose density differs from ρ_0 only in a central layer and is there piecewise constant. That solution can be adapted to the case in which $\nu = 0$ and $D = 0$ without difficulty. We include in figure 8 the resulting values of γ as a function of αl, for the simple density profile

$$\frac{\rho_1(z)}{\rho_0} = \begin{cases} 0, & |z| > l, \\ A, & |z| < l, \end{cases} \quad I = 2A^2 l. \tag{5.12}$$

Thus the asymptotic expression for γ for an arbitrary density profile, the result of a numerical calculation for a Gaussian profile, and the explicit analytical result for the piecewise-constant profile all coincide when $\alpha l \ll 1$, as expected. The values of γ for the two particular density profiles differ a little from each other when $\alpha l = O(1)$ because only at small values of αl is the effect of the density distribution represented by the parameter (5.9) used to make γ non-dimensional.

5.3. *Maximum growth rates of a disturbance* ($\nu \neq 0, D \neq 0$)

It appears from the analysis for an inviscid diffusionless fluid given above that the largest growth rates are associated with the more oscillatory disturbances having large values of α. Rayleigh–Taylor instability of inviscid fluid shows the same feature.

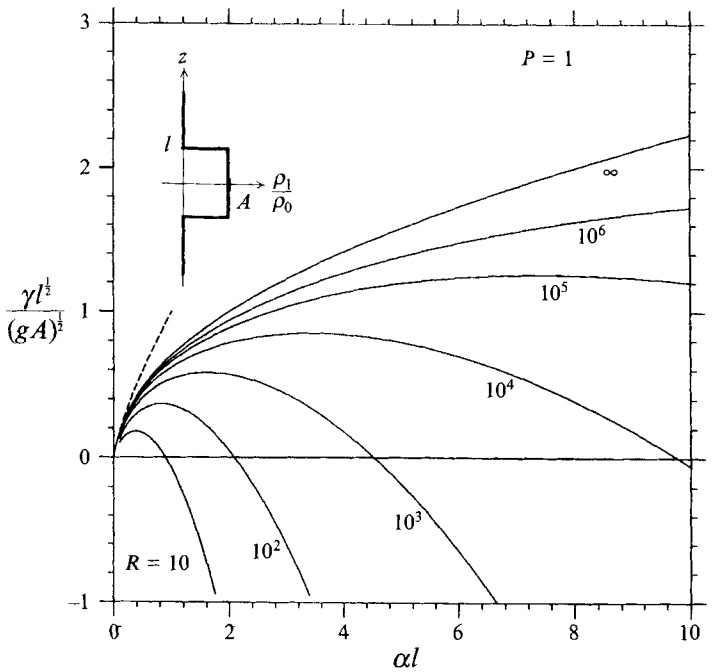

FIGURE 10. Growth rate γ as a function of αl for the piecewise-constant density profile (5.12) at several different values of $R(=2g|A|l^3/\nu D)$ according to the exact solution given in BN1 for unbounded fluid. The curve for $R\to\infty$ asymptotes to the relation (5.6) at $\alpha l \ll 1$ (shown as a broken line) and to the Rayleigh–Taylor relation (5.17) at $\alpha l \gg 1$.

However, viscous and diffusion effects will dampen the disturbance increasingly as α is increased. We may expect therefore that in reality there is a maximum of γ at some value of αl. The value of γ at its maximum and the value of αl at which it occurs, both as functions of R, represent useful pieces of information in any practical application. We now show that some of this information can be obtained from the known exact solution for a disturbance to unbounded fluid with a piecewise-constant density profile.

We must first recognize that the exact solution in question refers to infinite fluid without boundaries, whereas our objective in this paper has been to take account of the effect of a cylindrical boundary. However, the maximum value of γ in the case of unbounded fluid may be seen from figures 12(*b*), 12(*c*) and 12(*d*) in BN1 to occur at a value of αl which increases with the Rayleigh number; and the larger the number of oscillations of the disturbance along a horizontal line, the smaller will be the effect of the boundary. This was seen, for instance, in §3 where figure 1 shows that curves relating to bounded and unbounded fluid come together as the vertical wavenumber – which here specifies both vertical and horizontal lengthscales of the disturbance – increases relative to the cylinder radius. It is likely therefore that for large enough values of the Rayleigh number the maximum of γ occurs at a value of αl sufficiently far above unity for the effect of the presence of the boundary to be negligible. Judging by figure 1, the disturbance wavelength does not have to be much smaller than the horizontal dimension of the containing cylinder for the effect of the boundary to be small in the case of uniformly stratified fluid. A similar statement applies to the sinusoidal density variation considered in §4. For that case figure 6 shows that the minimum Rayleigh number corresponding to a given growth rate γ rapidly approaches the unbounded-fluid value with increasing κa.

The exact solution described in §6.2 of BN1 applies to undisturbed density profiles which are piecewise constant and to arbitrary values of the Rayleigh number. The key formula for the simple profile (5.12) having two discontinuities is equation (6.23) in that paper, namely

$$\frac{g\alpha^2|A|}{\nu D} = \{[f_0(0)]^2 - [f_0(2l)]^2\}^{-\frac{1}{2}}, \tag{5.13}$$

where, as set out in (6.4) of BN1,

$$f_0(z) = \frac{\nu D}{2\alpha\gamma^2}\left\{e^{-\alpha|z|} + \frac{P}{\sigma_1(1-P)}e^{-\sigma_1\alpha|z|} - \frac{1}{\sigma_2(1-P)}e^{-\sigma_2\alpha|z|}\right\} \tag{5.14}$$

and

$$\sigma_1 = \left(1+\frac{\gamma}{\alpha^2\nu}\right)^{\frac{1}{2}}, \quad \sigma_2 = \left(1+\frac{\gamma}{\alpha^2 D}\right)^{\frac{1}{2}}. \tag{5.15}$$

In figure 10 we show graphically the relation between $\gamma l^{\frac{1}{2}}/g^{\frac{1}{2}}A^{\frac{1}{2}}$ and αl for $P = 1$ and a number of different values of the Rayleigh number

$$R = 2g|A|l^3/\nu D$$

according to this exact solution. (For comparison with the two dotted curves in figure 12(*b*) of BN1, where the ordinate scale differs by the factor $R^{\frac{1}{2}}$, note that $|M_1|$ there is replaced by $2l|A|$ here.) The curve in figure 10 for the limit $R \to \infty$, corresponding to inviscid diffusionless fluid, may be seen from (5.13)–(5.15) to be given analytically by

$$\gamma^2 l/g|A| = \tfrac{1}{2}\alpha l(1-e^{-4\alpha l})^{\frac{1}{2}}. \tag{5.16}$$

When $\alpha l \ll 1$ the right-hand side of (5.16) reduces to $(\alpha l)^{\frac{3}{2}}$, thereby reproducing the expression for γ in (5.6) found from local analysis of inviscid motion in the central layer. And when $\alpha l \gg 1$, (5.16) reduces to

$$\gamma^2 \approx \tfrac{1}{2}\alpha g|A|, \tag{5.17}$$

which is the formula for the growth rate in Rayleigh–Taylor instability of an interface in inviscid fluid across which there is a density jump of non-dimensional magnitude $|A|$. This was to be expected because a disturbance of very short wavelength responds independently to the two interfaces specified in (5.12) (l now being irrelevant) and responds with growth at the one interface at which the heavier fluid is above lighter fluid.

At any finite value of R, the expression for $\gamma l^{\frac{1}{2}}/g^{\frac{1}{2}}|A|^{\frac{1}{2}}$ has a maximum at some value of αl and crosses the abscissa at a larger value of αl. It may readily be shown from the relations (5.13)–(5.15) that γ is zero at a value of αl which is given approximately by

$$(\alpha l)^3 = \frac{3}{32}R \tag{5.18}$$

as soon as $\alpha l > 1$. The value of αl at which γ is a maximum is not given conveniently by an explicit formula, but increases with R in a generally similar way as may be seen from the curves in figure 10. Note that l cancels from the two sides of (5.18), the layer thickness being irrelevant to the stability properties when $\alpha l \gg 1$. The smallest value of $|A|$ at which a neutral disturbance exists is related by (5.18) to the smallest value of α allowed by the boundary condition, which we saw in §5.1 to be of order a^{-1}.

The preceding powerful general solution holds for all values of the relevant parameters, but is restricted to piecewise-constant density distributions in the central layer. We shall give numerical results for one further such profile, namely

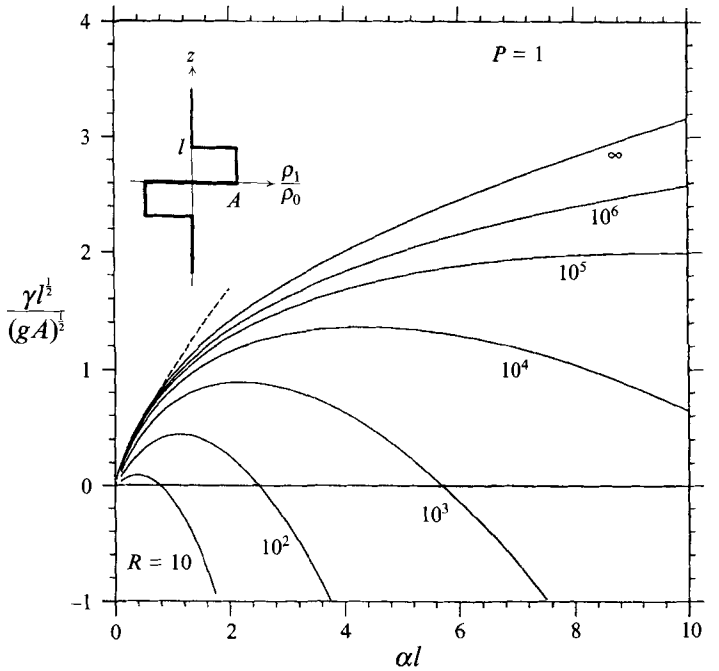

FIGURE 11. As for figure 10, but relating to the piecewise-constant density profile (5.19), for which the Rayleigh–Taylor asymptote at $\alpha l \gg 1$ is (5.20).

$$\frac{\rho_1(z)}{\rho_0} = \begin{cases} 0, & |z| > l \\ A, & 0 < z < l \\ -A, & -l < z < 0, \end{cases} \tag{5.19}$$

corresponding to what in BN1 was called a central layer of type (3′) if $A > 0$ (as will be supposed here). The explicit formula analogous to (5.13) is more complicated in this case. In figure 11 we show $\gamma l^{\frac{1}{2}}/g^{\frac{1}{2}}A^{\frac{1}{2}}$ as a function of αl for $P = 1$ and different values of R, defined again for convenience as $2gAl^3/\nu D$. The shapes of the curves are generally similar to those in figure 10, and in particular maxima occur at values of αl which increase with R. The asymptote for the curve corresponding to $R \to \infty$ at $\alpha l \ll 1$ is derived from (5.6) like that in figure 10, and the Rayleigh–Taylor asymptote at $\alpha l \gg 1$ is

$$\gamma^2 = \alpha g A, \tag{5.20}$$

which differs from (5.17) because the density jump at the central (unstable) interface is here $2A$. Note that the results are different when $A < 0$ (corresponding to a central layer of type 3).

6. A resumé of the two papers

We conclude with a brief review of what has been achieved in this paper and its predecessor BN1. The two papers together record an investigation of the behaviour of small disturbances to fluid of infinite vertical extent which initially is stationary and whose density varies in the vertical direction. The primary novelty of the problem lies in the fact that the undisturbed density gradient is zero on average over a large vertical range. The two basic types of density variation of this kind are (i) sinusoidal and (ii)

variation confined to a central layer. These density profiles have not been studied before, and necessitated the construction of mathematical methods *ab initio*. Insofar as the boundary is relevant we have assumed it to be a vertical rigid impermeable circular cylinder. Within this general specification of the project we have found a variety of mechanical processes and numerous new results for the growth rates of normal modes of disturbance. We have not restricted ourselves to specific objectives, and have felt free to explore interesting aspects of unstable behaviour and to formulate broad conclusions.

As a preliminary we have reviewed past work by Hales (1937), Taylor (1954), and Yih (1959) on the stability of uniformly stratified fluid in a long vertical tube and extended the ranges of values of the Rayleigh number and the vertical wavenumber (κ) of the disturbance for which the growth rate is known. In particular we have solved the governing equation for a neutral disturbance to find the Rayleigh number for given κa for each of the first three azimuthal modes of the disturbance in a circular tube. (This is, incidentally, the first solution for a disturbance which is neither axisymmetric nor two-dimensional nor z-independent, and it requires the satisfaction of an additional boundary condition and the determination of a fourth independent solution of the eigen-equation which is found to be connected with the vertical vorticity of the disturbance.) Although the first non-axisymmetric mode is neutral at a much smaller value of R than the axisymmetric mode when κa is of order unity or smaller, the difference between the critical Rayleigh numbers for the various azimuthal modes disappears when $\kappa a \gg 1$. At these large vertical wavenumbers there is a correspondingly small horizontal lengthscale of the disturbance, and the effect of the cylindrical boundary vanishes asymptotically, demonstrating the existence of a simple limiting state of which we make use in the case of other density profiles. We have also obtained numerical values of γ as a function of κa for various given values of R, including such large values that the fluid is effectively inviscid and diffusionless. At large values of κa there may be many combinations of κa, R and the sub-mode corresponding to the horizontal wavenumber of the disturbance which yield the same value of γ, requiring care in the identification of the disturbance with the largest growth rate at given R. An important reason for addressing here the case of constant density gradient is that it describes the asymptotic behaviour of systems with nonlinear undisturbed density profiles in the limit as the cylinder radius becomes much smaller than the vertical lengthscale over which the density varies.

The origin of the whole investigation was a speculation by one of us (Batchelor 1991) that, if a fluidized bed is unstable to plane waves of particle concentration with horizontal wave fronts, the continual increase in the amplitude of these waves will lead to a secondary or over-turning instability which will destroy the horizontal homogeneity. Confirmation of that hypothesis requires a consideration of two-phase flow, and in preparation for that we have here asked whether a sinusoidal vertical distribution of fluid density is unstable and if so what is the form of the disturbance that grows most rapidly. The answer is not obvious, and we did not anticipate finding that in unbounded fluid (§5, BN1) a disturbance of sufficiently large horizontal wavelength will grow exponentially at any amplitude of the sinusoidal density variation. The nature of the disturbance motion is also interesting; the velocity associated with a disturbance of large horizontal wavelength is approximately vertical everywhere and tilts the alternate layers of heavier and lighter fluid, causing the heavier layers to slide down and the lighter fluid to slide up, leading in turn to a periodic horizontal variation of the vertically averaged density and thereby to reinforcement of the vertical motion. This efficient process for the release of potential energy of the fluid

operates at all Rayleigh numbers, including large values at which ν and D are effectively zero. In this latter case each initially horizontal thin lamina of fluid slides independently, and a simple local analysis recovers the asymptotic expression for γ (and is applicable to the more general case of an undisturbed density which is a periodic but not necessarily sinusoidal function of z).

It is surprising that the stability of a sinusoidal density profile has not previously been investigated. This may be because others have been less willing to adopt our assumption that the change with time in the basic density distribution due to diffusion may be neglected. We cannot justify this assumption in general, but there are undoubtedly situations in which small values of the diffusivity are relevant, or in which there is no effect of diffusion on the particular parameter of the density distribution that is relevant to instability, or (as in the case of a fluidized bed) there is another physical process in operation (namely particle inertia) which can bring about a constant form of the density variation despite the smoothing effect of particle diffusion.

The smallest value of the Rayleigh number $R(= gA/\kappa^3\nu D)$ at which a neutral disturbance with horizontal wavenumber α in unbounded fluid with a sinusoidal density profile exists tends to $\sqrt{2}\alpha/\kappa$ as $\alpha/\kappa \to 0$. However, in the presence of a cylindrical boundary α is no longer arbitrary and must be determined from the boundary conditions. This changes the nature of the relation between R and κa for a neutral disturbance, although not in the limit $\kappa a \to \infty$. At the other extreme, $\kappa a \to 0$, the boundary dominates the behaviour of the disturbance, and the smallest uniform density gradient in fluid in a vertical tube at which a neutral disturbance exists is the same as the critical value of the density gradient at the place in a sinusoidal profile in the tube where the gradient is a maximum. Our numerical finite-difference solution for the r-dependence of a disturbance (the dependence on z and θ being represented by Fourier series) reveals these limiting forms of behaviour explicitly.

Although we do not know of any direct practical application, we think the problem of stability of a central horizontal layer in which the fluid density departs from its uniform value outside the layer is of sufficient intrinsic interest to justify the investigation described in the two papers. Mathematically it has some features in common with the stability of a transition layer between two regions of different density; and the tilting–sliding mechanism of instability is relevant when $\alpha l \ll 1$. We have explored several mathematical methods, applicable under different conditions, and will single out one for mention here in view of its unusual power. This method gives the exact solution for the case of a piecewise-constant density profile as well as asymptotic solutions for arbitrary density profiles in unbounded fluid. It begins with Fourier transformation of all terms in the governing equation for $W(z)$ (see (6.1) in BN1). For piecewise-constant density profiles the convolution integral contains the product of the density gradient, which is a sum of delta functions, and $W(z)$. Inversion and use of an identity established by contour integration then leads, remarkably, to an exact solution in closed form for any value of γ, R and αl. This solution remains valid, approximately, in the presence of a cylindrical boundary provided $l/a \ll 1$.

Appendix: Proof that $\kappa = 0$ gives the minimum critical Rayleigh number in the case of constant density gradient

By M. R. E. Proctor
Department of Applied Mathematics and Theoretical Physics,
University of Cambridge, Silver Street, Cambridge CB3 9EW, UK

We begin with equations (2.1)–(2.3) and consider an arbitrary cylindrical container with generators parallel to the vertical z-axis and of infinite length in the z-direction. We suppose that l is a characteristic horizontal dimension of the cylinder, and that the undisturbed density gradient $\mathrm{d}\rho_1/\mathrm{d}z$ is $\rho_0\beta$ where β is a positive constant. Then scaling lengths with l, velocities with D/l, time with l^2/D, ρ' with $\beta l\rho_0$ and p' with $\rho_0\nu D/l^2$, we obtain the dimensionless equations

$$\nabla\cdot\boldsymbol{u} = 0, \tag{A 1}$$

$$\sigma^{-1}\frac{\partial \boldsymbol{u}}{\partial t} = -R\hat{\boldsymbol{z}}\rho' - \nabla p' + \nabla^2\boldsymbol{u}, \tag{A 2}$$

$$\frac{\partial \rho'}{\partial t} + w = \nabla^2\rho', \tag{A 3}$$

where $\sigma = \nu/D$ and the Rayleigh number $R = |\boldsymbol{g}|\beta l^4/D\nu$.

If we seek steady solutions that are periodic in z with period $2\pi/\kappa$ we may set the time derivative terms in (A 2)–(A 3) equal to zero. It may then be seen, by using the boundary conditions (2.7), that R may be written as the homogeneous functional

$$R = \frac{\langle|\nabla\rho'|^2\rangle\langle|\nabla\boldsymbol{u}|^2\rangle}{\langle|\rho' w|\rangle^2} \tag{A 4}$$

where the bracket denotes an average over the cylinder:

$$\langle . \rangle \equiv \frac{\kappa}{2\pi A}\int_0^{2\pi/\kappa}\mathrm{d}z\iint_A \mathrm{d}x\,\mathrm{d}y(.) \tag{A 5}$$

and A is the cross-sectional area of the cylinder in the (x, y)-plane. Elementary calculus of variations then shows that the Euler–Lagrange equations for the extrema of the functional (A 4) with respect to variations of $\boldsymbol{u}, \rho'$ that preserve the boundary conditions (2.7) and the incompressibility constraint (2.1) are in fact identical with (A 2), (A 3) (with $\partial/\partial t = 0$). Thus the eigenvalues R are extrema of (A 4) and the minimum $R_{min}(\kappa)$ gives the smallest Rayleigh number for a neutral disturbance.

Now select a trial function $(\hat{\boldsymbol{u}}, \hat{\rho})$ satisfying (2.7) and denote the value of R for this trial function by $\hat{R}$. Then we have

$$\hat{R} \geqslant \frac{\langle|\nabla\hat{\rho}|^2\rangle\langle|\nabla\hat{w}|^2\rangle}{\langle|\hat{\rho}\hat{w}|\rangle^2} \geqslant \frac{\langle|\nabla_h\hat{\rho}|^2\rangle\langle|\nabla_h\hat{w}|^2\rangle}{\langle|\hat{\rho}\hat{w}|\rangle^2} \equiv \hat{S}. \tag{A 6}$$

Thus $\hat{R} \geqslant \hat{S}$ for any trial function, and so $\hat{R} \geqslant S_{min}$, where S_{min} is the minimum of $\hat{S}$ as $\hat{\rho}, \hat{w}$ are varied over all functions satisfying $\boldsymbol{n}\cdot\nabla\hat{\rho} = \hat{w} = 0$ on the cylinder walls. (These conditions are certainly contained in (2.7) and $\hat{w}$ is now less constrained since $\nabla\cdot\hat{\boldsymbol{u}} = 0$ is not imposed.) Thus, since $(\hat{\boldsymbol{u}}, \hat{\rho})$ are arbitrary, S_{min} certainly gives a lower bound on the critical value R_{min}. But the Euler–Lagrange equations for the extrema of $\hat{S}$ contain no z-derivatives, and are satisfied by the steady solutions of (A 1)–(A 3) which are independent of z (in which case $\boldsymbol{u}_h \equiv 0$ and (A 1) is trivially satisfied). Thus S_{min}, which is in fact $R_{min}(0)$, is also the minimum of $R_{min}(\kappa)$ as κ is varied, and this is the result that was to be proved.

In the case that the bounding cylinder is circular in cross-section, the equations can be separated in the azimuthal coordinate θ, and one can study a separate stability problem for solutions of the form $e^{\pm in\theta}$ for every integer n. It is easy to see that the arguments of the preceding paragraph can be adapted to this case, so that we can assert that, for each n, $\kappa = 0$ gives the lowest critical Rayleigh number. This result makes it possible to obtain simple expressions for the critical numbers for every n, since the solution of the governing equations is straightforward when $\kappa = 0$.

REFERENCES

BATCHELOR, G. K. 1991 The formation of bubbles in fluidized beds. In *Of Fluid Mechanics and Related Matters, Proc. Symp. Honoring John W. Miles on his 70th Birthday*, pp. 29–44. Scripps Institution of Oceanography, Reference Series 91–24.

BATCHELOR, G. K. & NITSCHE, J. M. 1991 Instability of stationary unbounded stratified fluid. *J. Fluid Mech.* **227**, 357–391 (referred to herein as BN1).

CHANDRASEKHAR, S. 1961 *Hydrodynamic and Hydromagnetic Stability*. Oxford University Press.

DONGARRA, J. J. & MOLER, C. B. 1984 EISPACK – a package for solving matrix eigenvalue problems. *Argonne National Laboratory, Math. & Comp. Sci. Div., Tech. Memo.*

HALES, A. L. 1937 Convection currents in geysers. *Mon. Not. R. Astron. Soc., Geophys. Suppl.* **4**, 122.

JONES, C. A. & MOORE, D. R. 1979 The stability of axisymmetric convection. *Geophys. Astrophys. Fluid Dyn.* **11**, 245–270.

TAYLOR, G. I. 1954 Diffusion and mass transport in tubes. *Proc. Phys. Soc.* B **67**, 857–869.

YIH, C.-S. 1959 Thermal instability of viscous fluids. *Q. Appl. Maths* **17**, 25–42.